TEM image simulation

Pierre Stadelmann
CIME-EPFL
CH-1015 Lausanne
Switzerland
Pierre.Stadelmann@epfl.ch

June 3, 2012

Introduction

The formation of Transmission Electron Microscopy (TEM) images involves complex physical processes that are characterized and modeled in order to perform computer simulations. There is no unique set of approximations that allows to model and calculate the numerous sorts of images that a TEM provides (in a more or less reasonable cpu time).

The approximations, assumed by the modeling process are strongly, dependent on the images to be simulated (SAED, CBED, LACBED or PED diffraction, HRTEM, Weak Beam, Hologram, ...). In this document we will describe some of them relevant to the simulation of diffraction patterns and high resolution TEM images.

Prior to perform any calculation the following items (from the electron source to the detector) must characterized and modeled:

- The electron beam properties.
- The specimen properties[1].
- How is the incident electrons scattered by the specimen?
- How does the microscope transfer the scattered electron beam?
- How do we measure the properties of the scattered electron beam (diffraction, image, hologram)?

[1] file://localhost/Users/pierrestadelmann/Desktop/HamiltonJune2012/html/Rb2WO9/Rb2WO9.html

Modeling of TEM operation

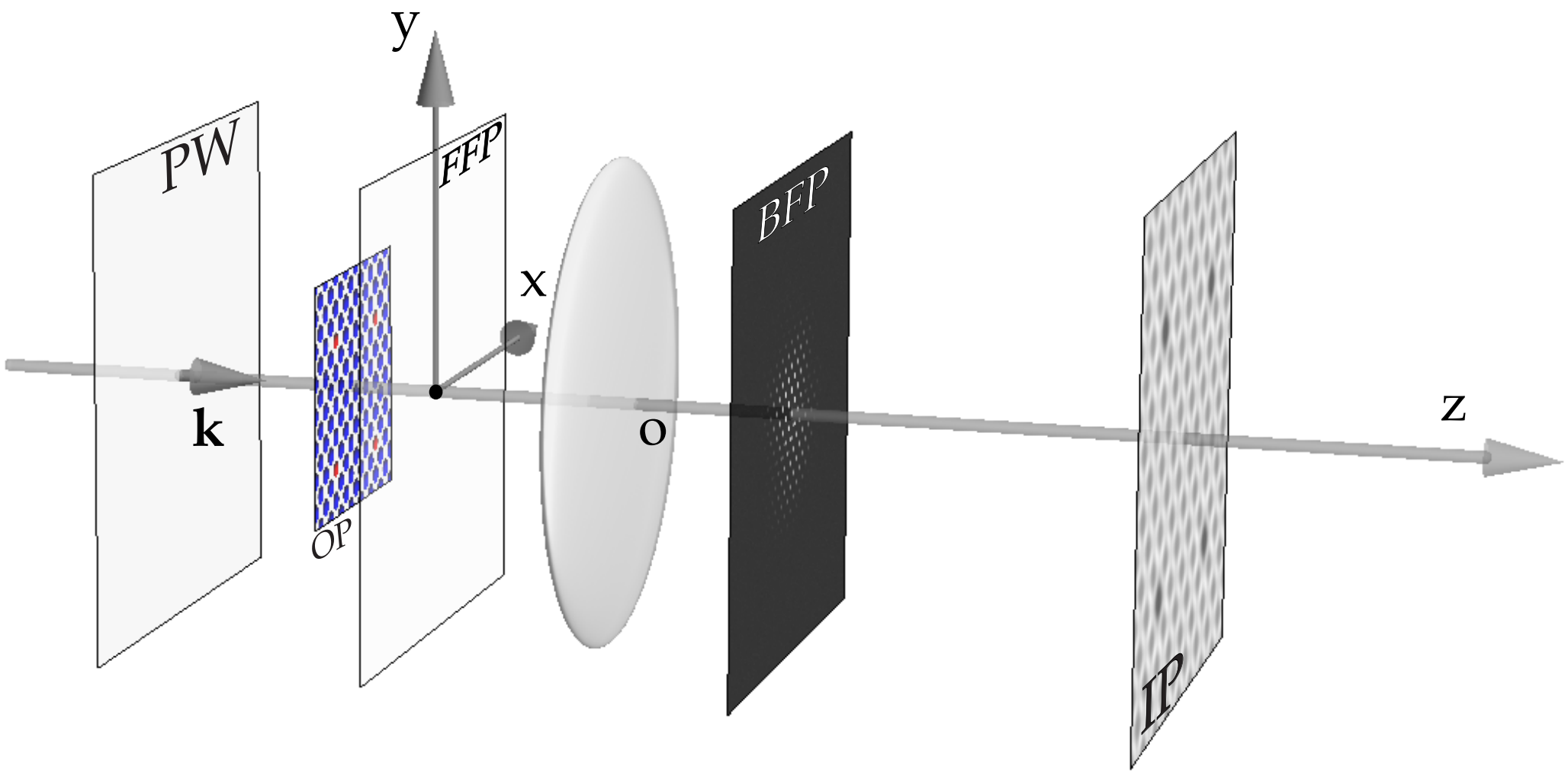

Modeling steps: Incident wave, crystal, electron-matter interaction, Fraunhofer approximation, image formation.

Diffraction pattern depends on specimen thickness

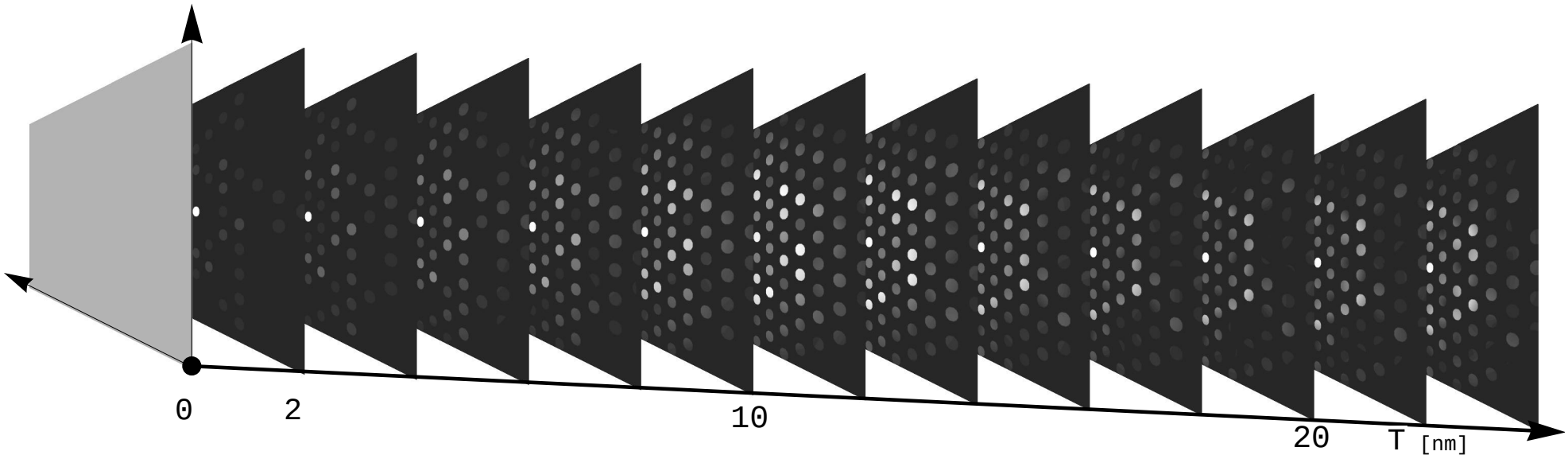

Dynamical diffraction

HRTEM image depends on specimen thickness and object defocus

Thickness series

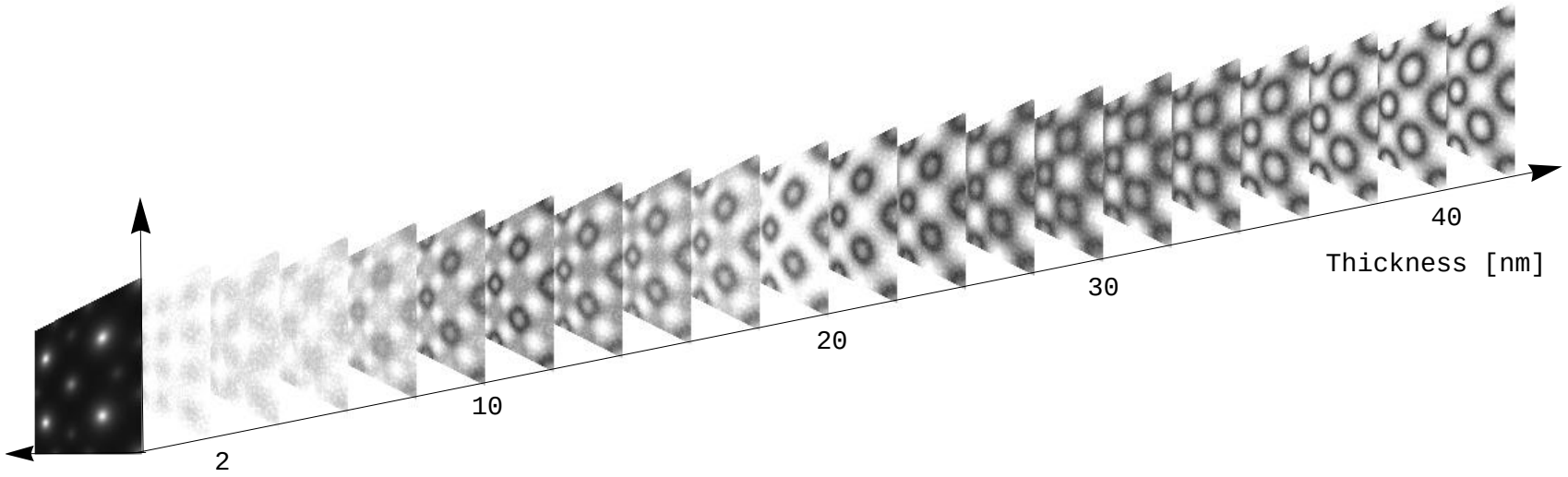

Defocus series

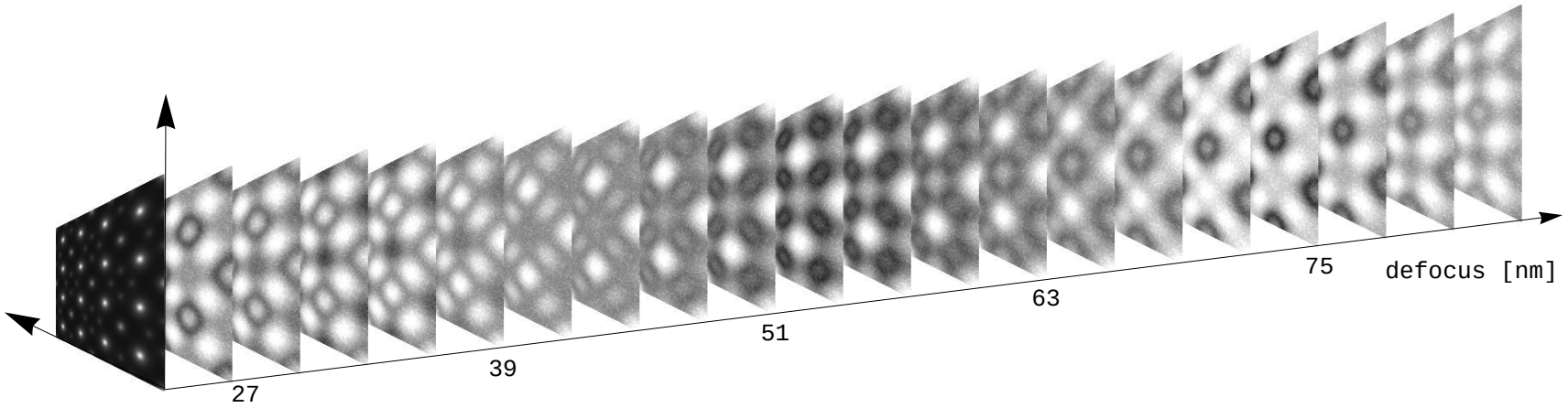

HREM map to show defocus - thickness dependence

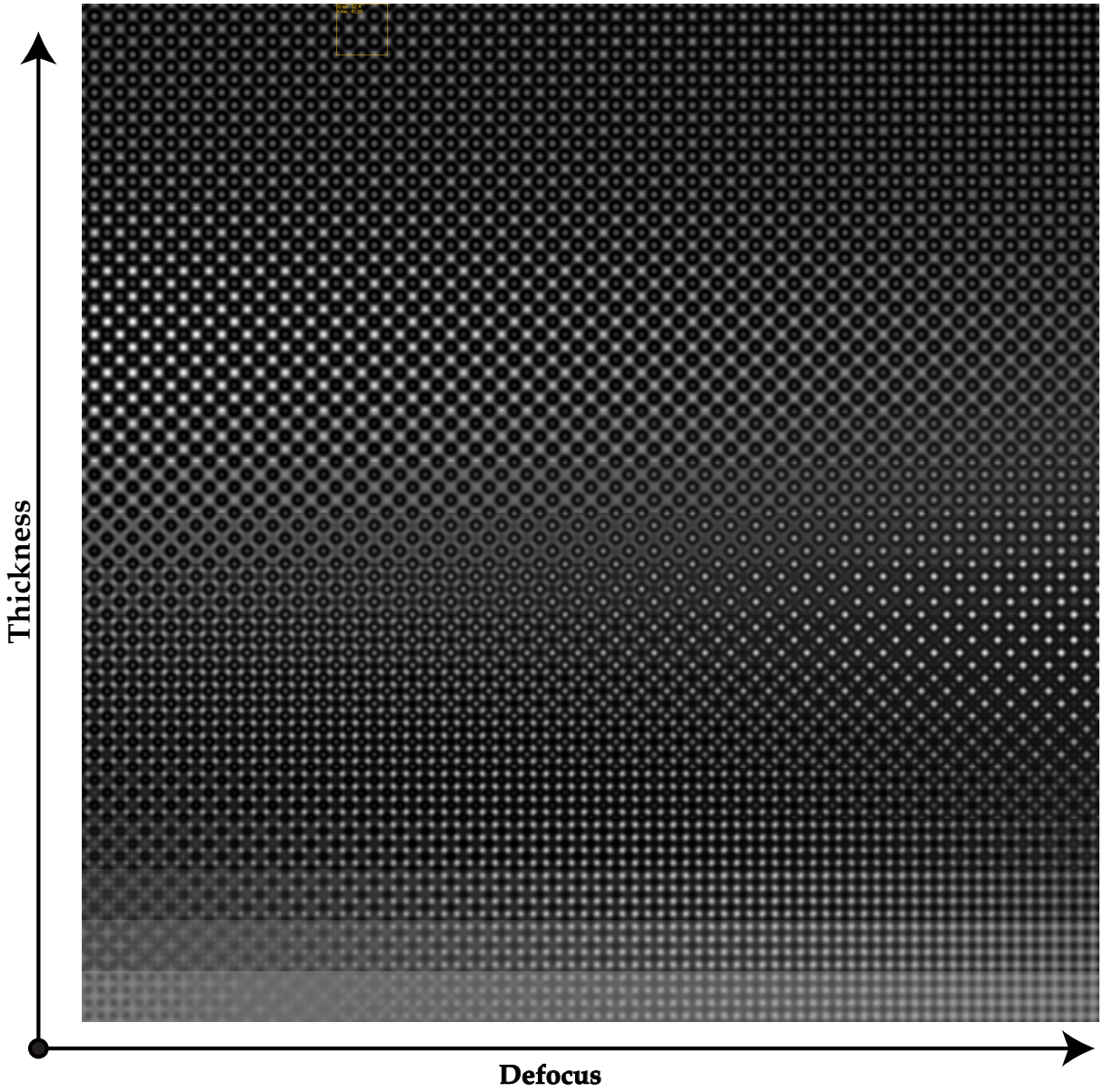

HREM map does not include the Modulation Transfer Function (MTF) of the detector[2].

[2] See discussion of detector MTF below page 52.

First modeling decision

The first modeling decision concerns the representation of a plane wave:

- Crystallography and optics: $\Psi(\vec{r}) = e^{2i\pi\vec{k}\,.\,\vec{r}}$.
- Quantum mechanics: $\Psi(\vec{r}) = e^{i\vec{k}\,.\,\vec{r}}$.

This choice as consequences for all the future modeling steps, in particular the description of the transfer function of the microscope and the controversial sign of the objective lens defocus[3].

This choice determines also the choice of the phase shift of the transfer function of the objective lens and of the **underfocus** parameter[4].

[3] L. Reimer, *"Transmission Electron Microscopy"*, Springer-Verlag 1993.

[4] See discussion on page 9.

Microscope modeling: Abbe image formation theory

The objective lens is modeled as a thin lens that brings the Fraunhofer diffraction pattern at a finite distance (i.e. in its back focal plane).

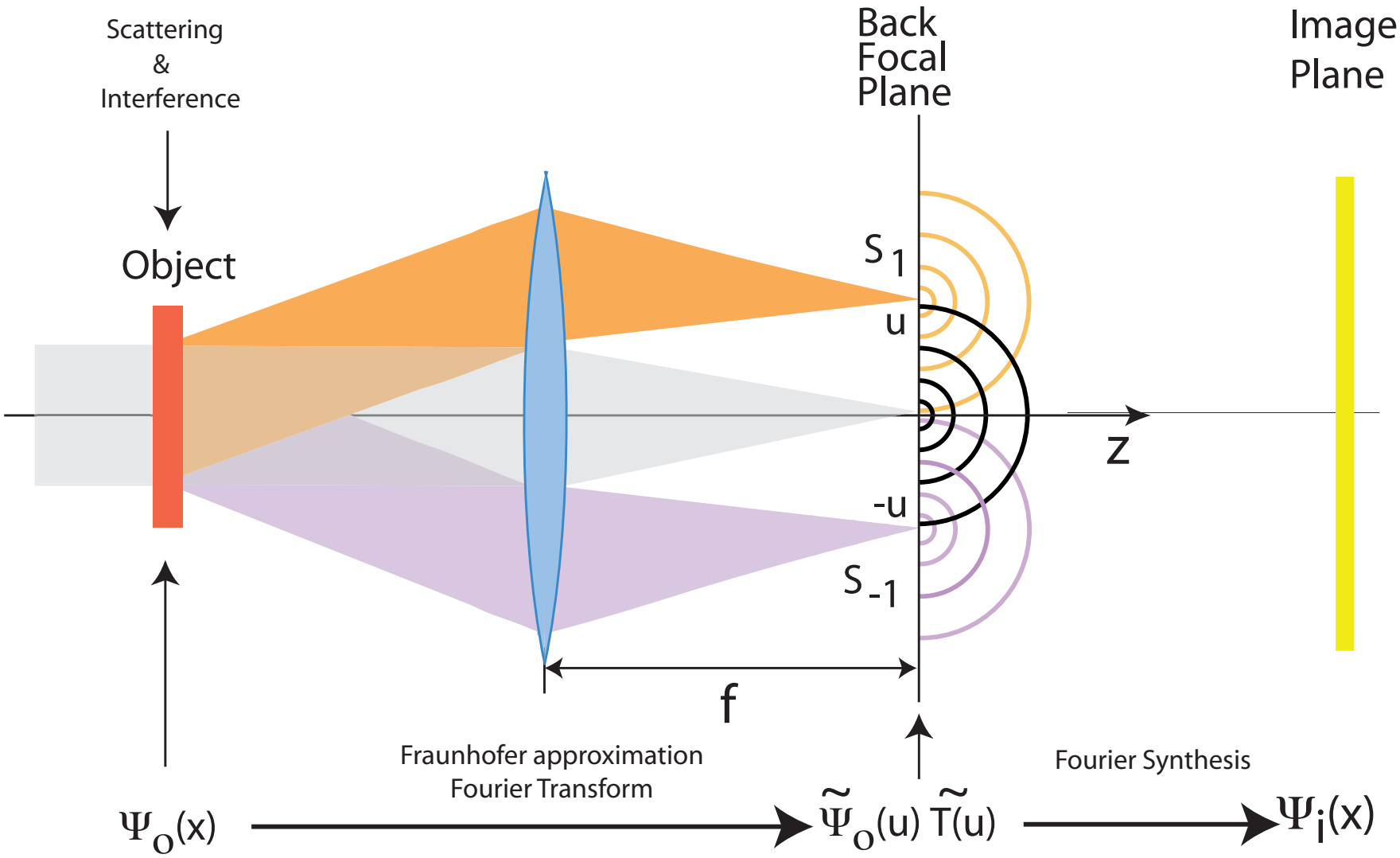

Paraxial optics: perfect thin lens

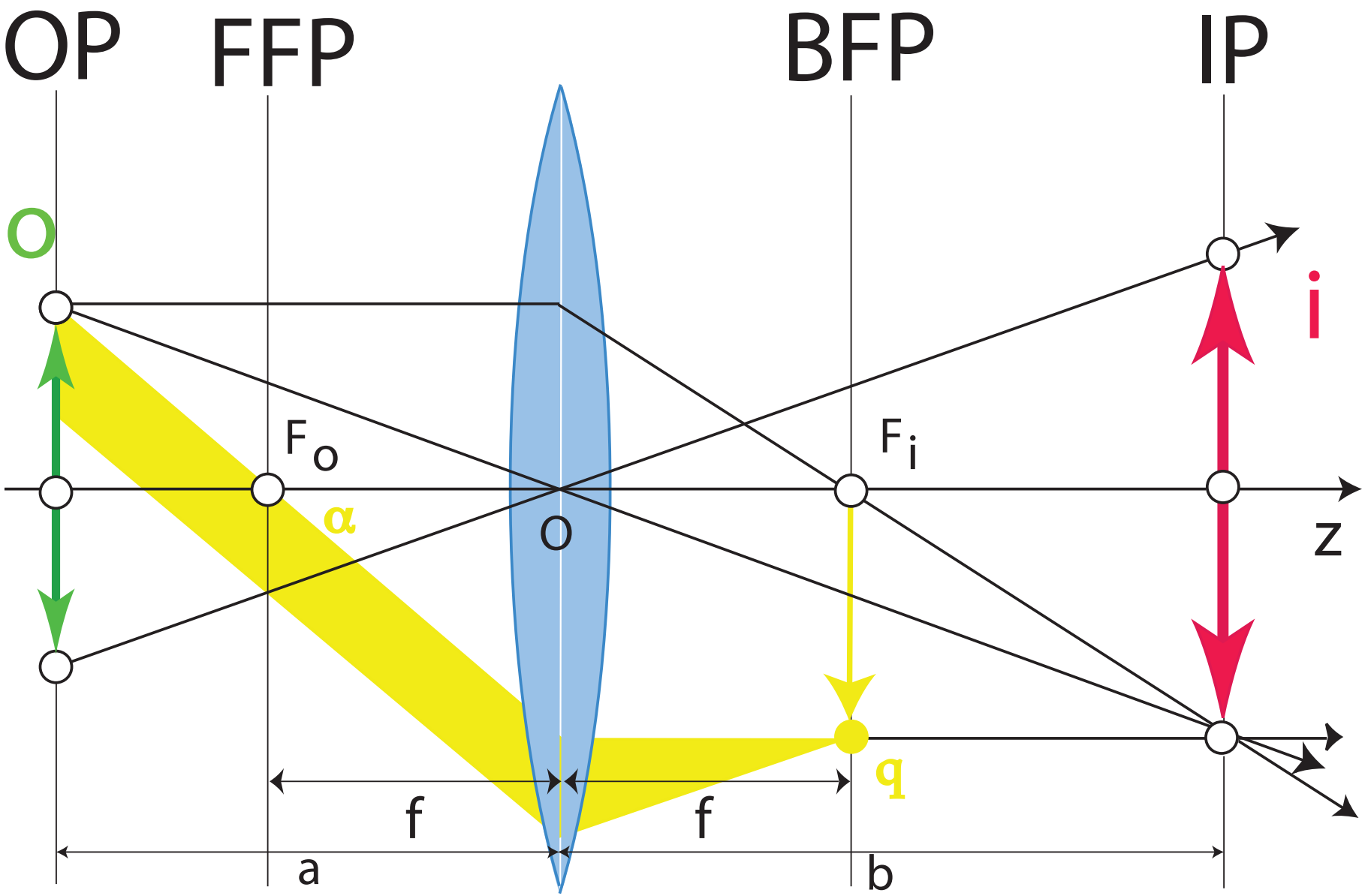

Principal rays of paraxial optics. Reflection (plane wave) making an angle α, where $\alpha = 2\theta_B$, corresponds to spatial frequency q.

Optical Path Length: spherical aberration

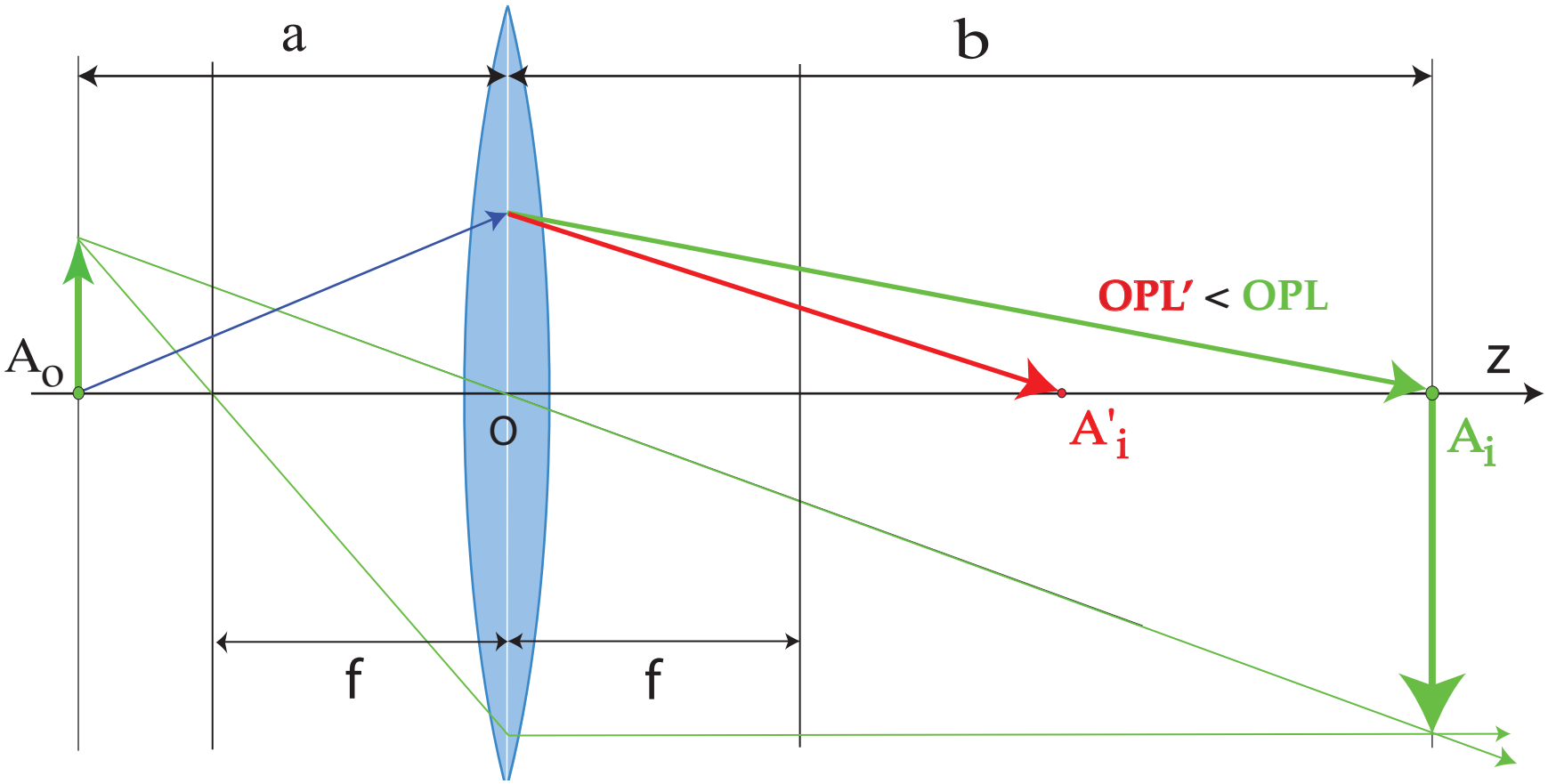

In presence of spherical aberration, the optical path length (OPL') form A_o to A'_i is smaller than OPL from A_o to A_i. The wavefront at A'_i is out-of-phase by[5]:

$$e^{-2\pi i \frac{C_s \lambda^3 (\vec{q}\cdot\vec{q})^2}{4}}$$

[5]With our plane wave choice.

Optical Path Length: underfocus

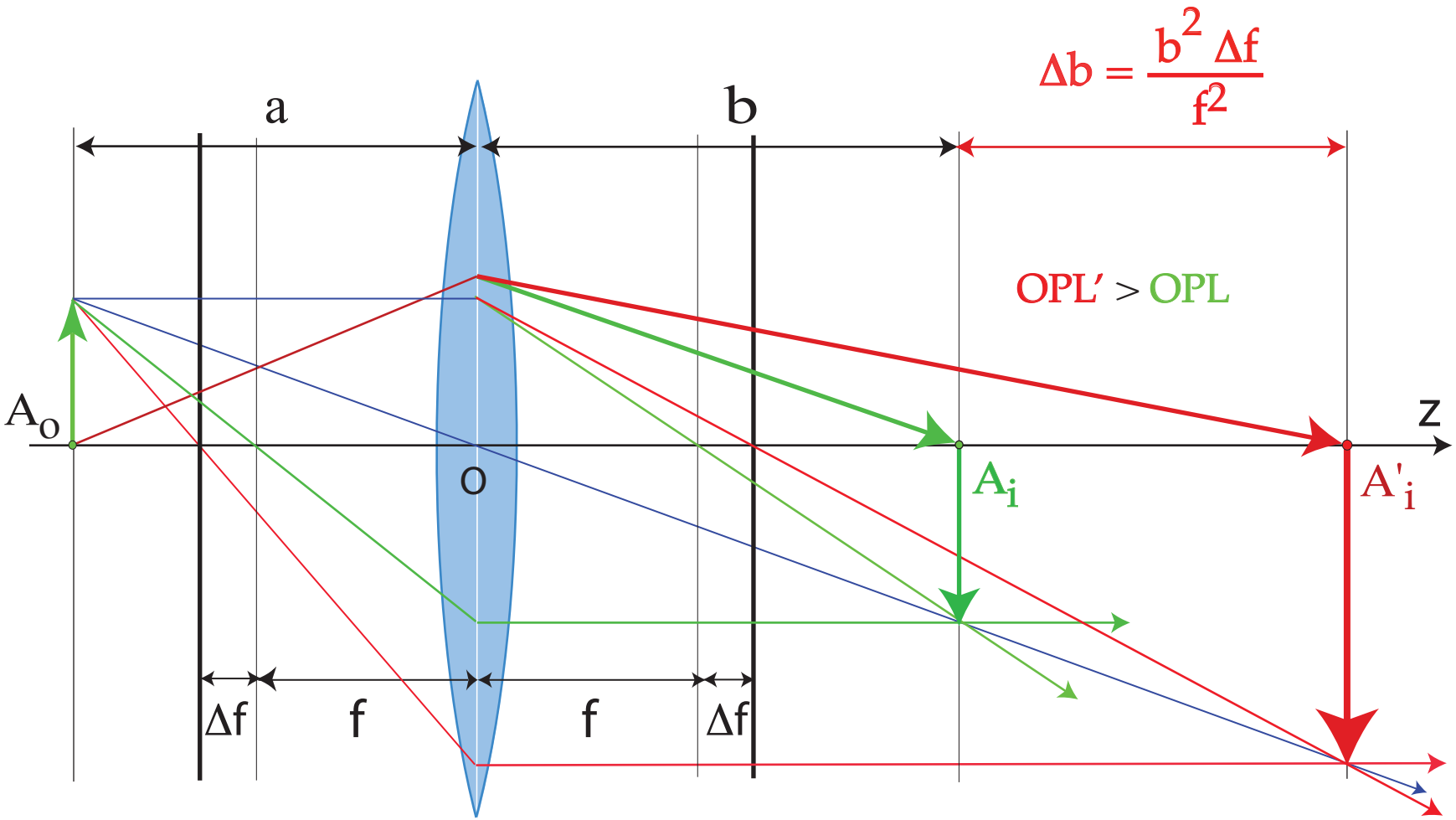

Underfocus weakens the objective lens, i.e. increases f. As a consequence the OPL from A_o to A'_i is larger:

$$e^{2\pi i \frac{\Delta f \lambda (\vec{q}\cdot\vec{q})}{2}}$$

Optical Path Length: eucentricity

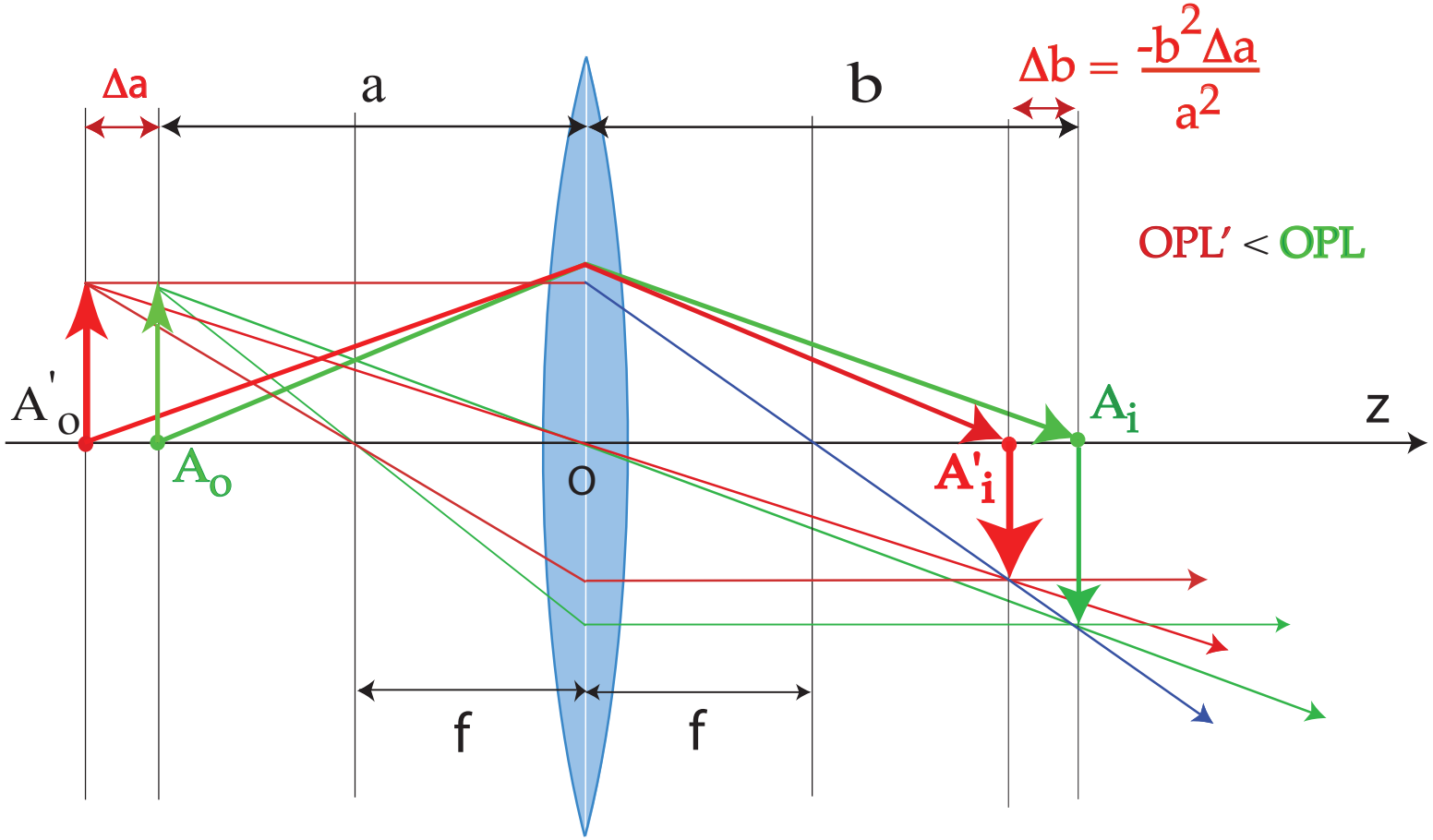

On the contrary keeping f constant and moving the object by Δa decreases the OPL.

Transfer function of the objective lens

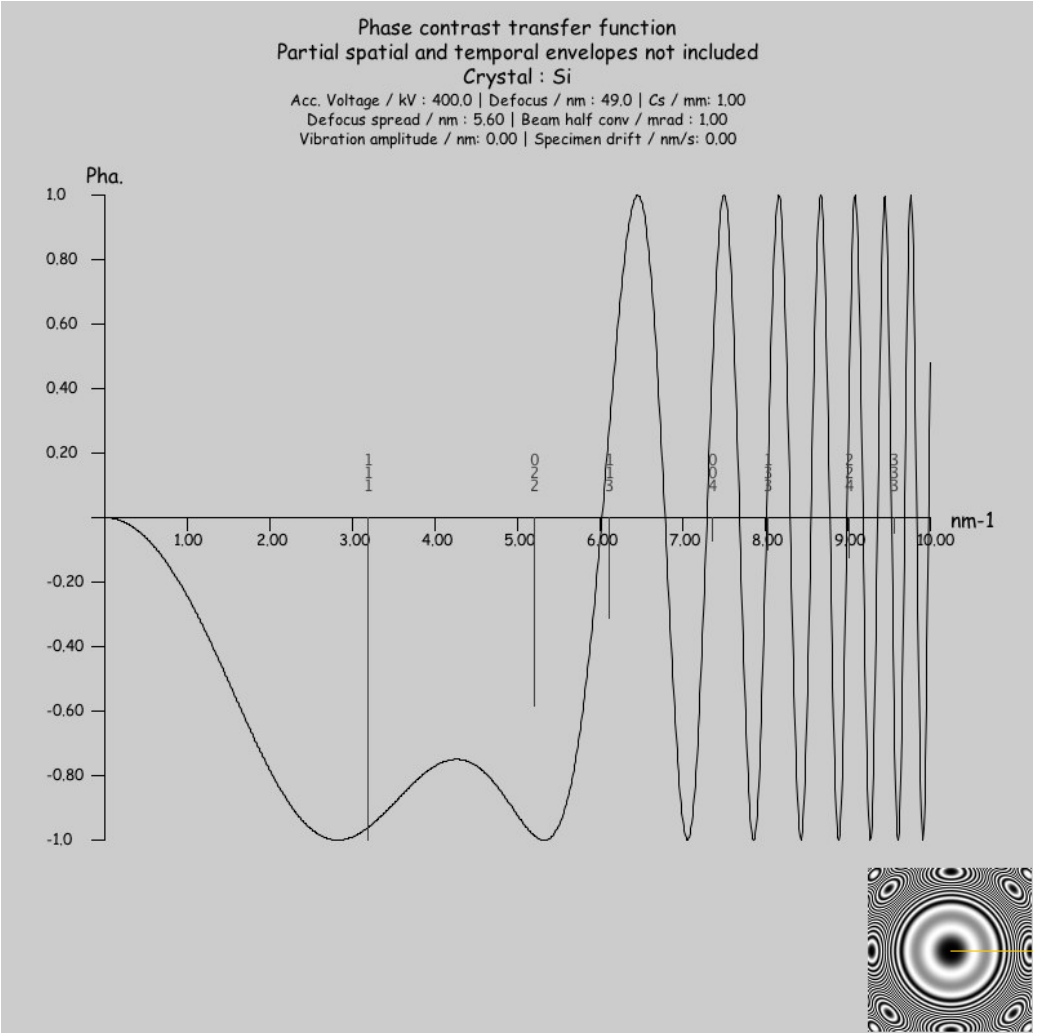

The transfer function of the objective lens in the absence of lens current and accelerating voltage fluctuations (Scherzer defocus). The (111) and (022) reflections of Si are phase shifted by $-\frac{\pi}{2} \rightarrow$ black atomic columns.

Electron beam properties

1. Energy (E).
2. Energy dispersion or spread (ΔE).
3. Momentum dispersion or angular spread (ΔK).

These properties allow to describe the spatial and temporal coherence of the incident electron wave which are extremely important in high resolution imaging[6].

[6] K. Ishizuka, *"Contrast Transfer of Crystal Images in TEM"*, Ultramicroscopy 5 (1980) 55.

Constants

c = speed of light in vacuum.
e = electron charge.
E = accelerating voltage ($\geq 50kV$).
$\gamma = 1 + \frac{e^2\ E^2}{2\ m_0\ c^2}$ (relativistic mass correction).
m_0 = rest mass of the electron ($\approx 511\ keV$).

$E\,[kV]$	γ	$\lambda\,[pm]$	$\frac{v}{c}$
50	1.098	5.362	0.412
100	1.119	3.706	0.548
200	1.391	2.511	0.695
500	1.978	1.423	0.862
1000	2.957	0.873	0.941

Relativistic mass correction, wavelength and speed of the electron.

Coherence of the electron beam

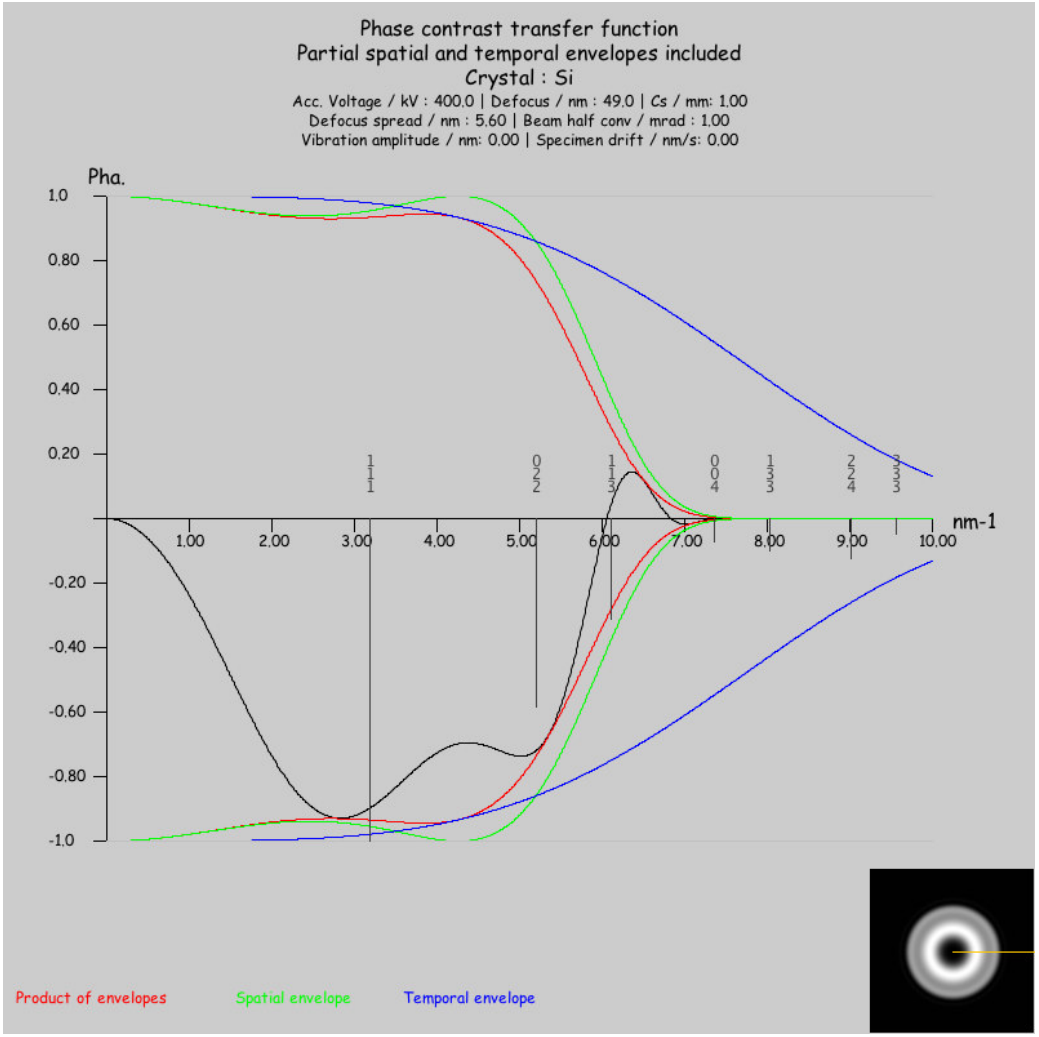

Partial spatial and temporal coherence of the electron beam introduce an attenuation of the transfer of high spatial frequencies.

Specimen properties

1. Amorphous material or crystalline material.
2. Thin or thick.
3. Orientation (high or low symmetry [uvw]).

You might have to transform the unit cell in order to perform the dynamical calculations[7].

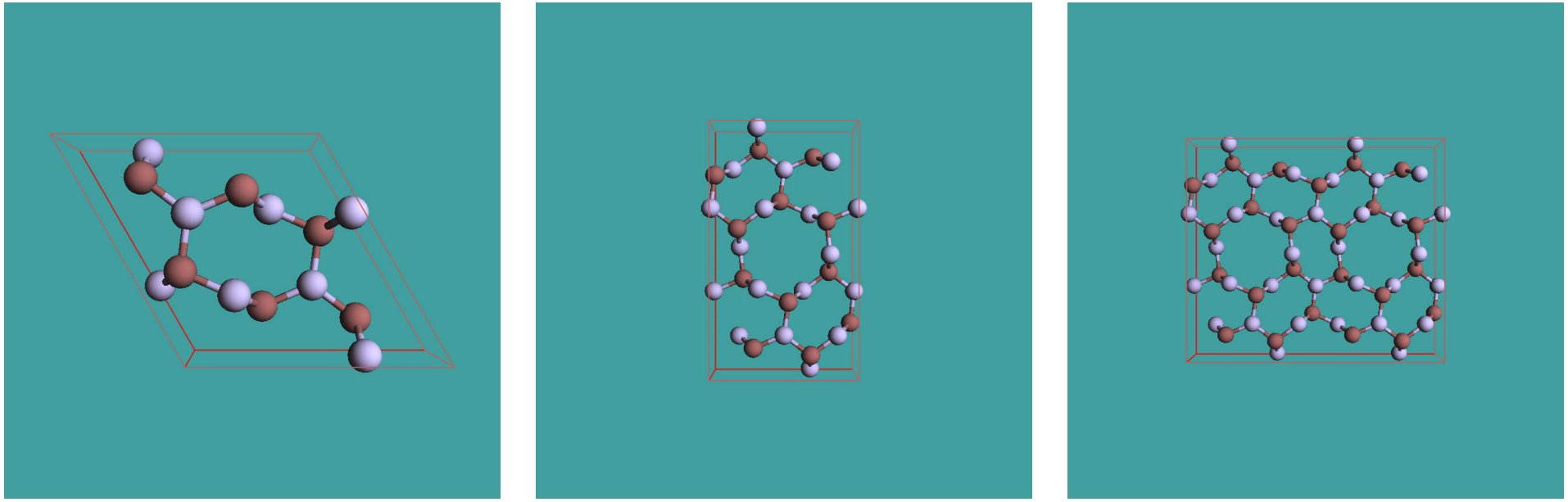

A: Si_3N_4 hexagonal lattice. B: Si_3N_4 orthorhombic lattice. C: Si_3N_4 orthorhombic lattice x 2.

[7] See International Tables for Crystallography (1992) Vol. 1, Chapter 5.

Atomic form factors

Atomic form factors have been tabulated by many authors:

1. Doyle-Turner and Smith-Burge.
2. E.J. Kirkland.
3. Peng-Ren-Dudarev-Whelan.
4. ...

Take care ASA of heavy atoms aren't always tabulated properly.

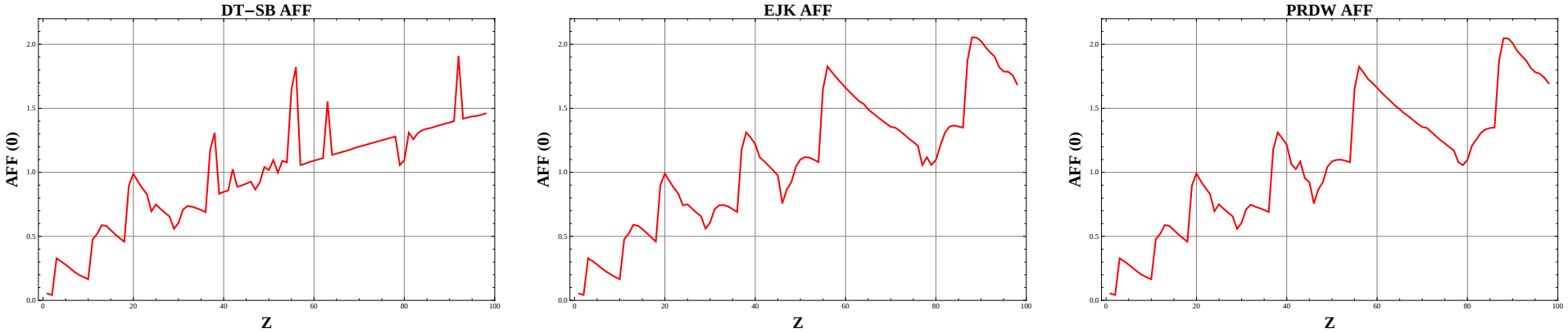

A extremely useful ASA tabulation including phonon and core loss absorption is due to Weickenmeier-Kohl[8].

[8] A. Weickenmeier, H. Kohl, Acta Cryst. A 47 (1991) 590.

Diffraction geometry

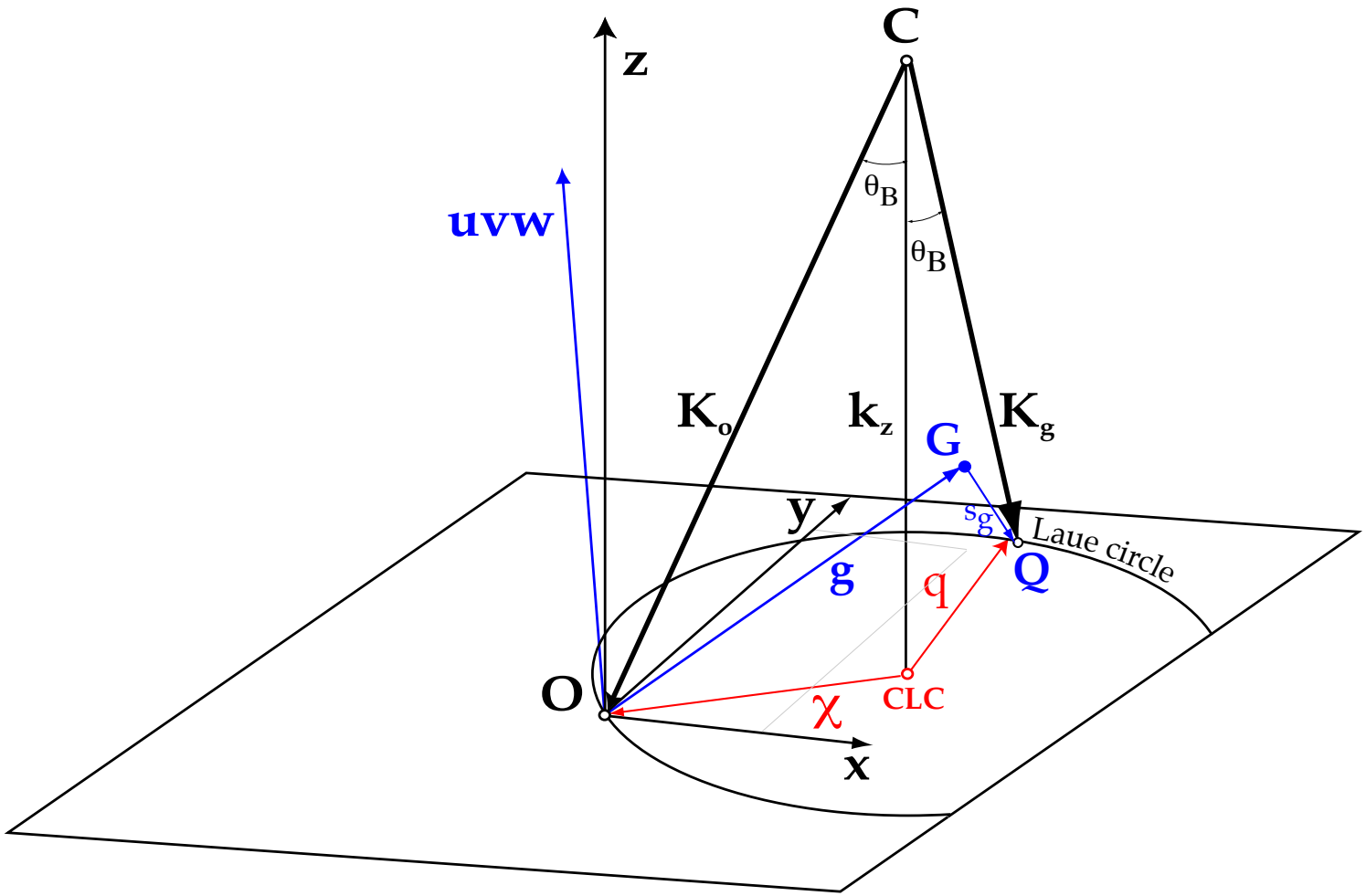

Center of the Ewald sphere (C) and Center of the Laue Circle (CLC), projection of C onto the zero order Laue zone. All reflections on the circle of radius χ are at exact Bragg condition.

Typical Bragg angles

At 100 kV, Bragg angles for several reflections of Al are given in the next table.

(hkl)	*Bragg angle* $[mrad]$	*Bragg angle* $[deg.]$	(hkl) *spacing* nm^{-1}
(1,1,1)	7.91	0.453	4.276
(2,0,0)	9.14	0.523	4.938
(2,2,0)	12.92	0.740	6.983
(1,1,3)	15.15	0.868	8.189
(2,2,2)	15.83	0.906	8.553
(4,0,0)	18.28	1.047	9.876

Bragg angles for some Al reflections at 100 kV.

Notice that the Bragg angles are pretty small (of the order a few ^{o}) and that consequently the small angle approximation is quite good.

Electron-matter interaction

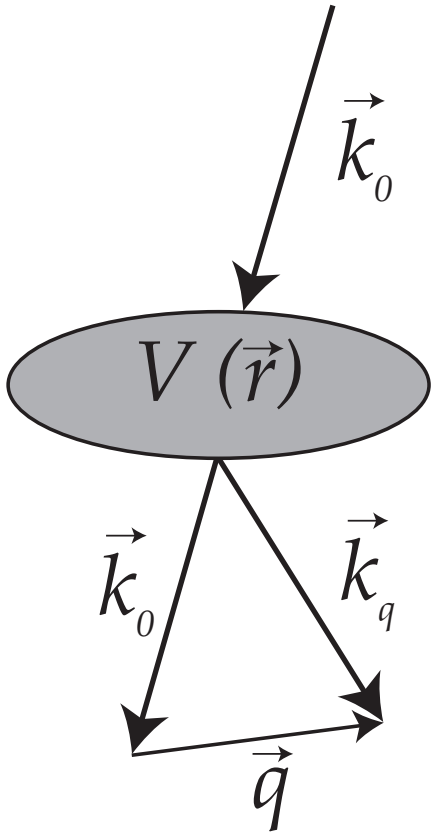

An incident electron of wave vector $\vec{k}_0$ interacts with a solid of scalar potential $V(\vec{r})$. The wave vector of the scattered electron is $\vec{k}_q = \vec{k}_0 + \vec{q}$ where $\vec{q}$ is the momentum transfered by the solid[9].

[9] Magnetic and spin effects are ignored.

Approximations: elastic scattering of high energy electrons

Elastic scattering:

- Energy conservation ($\Delta E = 0$).
- Momentum transfer ($q \geq 0$).
- Scattering of high energy electrons (i.e. electrons accelerated by potential $\geq 50\ kV$):
  - $\Longrightarrow$ electrons scattered at small angles (few degrees).
- Strong electron-matter interaction (10^4 times larger X-rays):
  - $\Longrightarrow$ very thin crystals only can be imaged.
  - $\Longrightarrow$ Relaxed Bragg condition (reciprocal rod - many reflections).

$\vec{k_i}$: incident wavevector

$\vec{k_g}$: scattered wavevector

$\vec{g}$: reciprocal lattice vector

$\vec{s_g}$: deviation from exact Bragg condition

1. Energy conservation: $|\vec{k_g}| = |\vec{k_i}|$.
2. Momentum transfer: $\vec{k_i} + \vec{g} + \vec{s_g} = \vec{k_g}$.

Bragg law

With energy conservation and momentum transfer ($\vec{s_g} = 0$):

$$|\vec{k_i} + \vec{g}| = |\vec{k_g}|$$

$$k_i^2 + 2 \times k_i \times g \times \cos(\vec{k_i}, \vec{g}) + g^2 = k_g^2$$

$$2k_i \times \cos(\vec{k_i}, \vec{g}) = -g$$

$$2k_i \times \cos(90^o - \theta_B) = -g$$

$$\frac{2}{\lambda} \times \sin(\theta_B) = g = \frac{1}{d_g}$$

$\Longrightarrow$ Bragg law:

$$2 \times d_{hkl} \times \sin(\theta_B) = \lambda$$

Intensity in the single scattering approximation: kinematic theory

Kinematically the intensity of any reflection (or diffracted spot as observed on a CCD camera) is proportional to I_{hkl}:

$$I_{hkl} = F^*_{hkl} F_{hkl}$$

where the structure factor F_{hkl} is:

$$F_{hkl} = \sum_{i=atoms} f_i(hkl) \exp^{-[2\imath\pi(hx_i+ky_i+lz_i)]} \; occ_i \; DW_i(hkl)$$

$\Rightarrow$ **Single scattering approximation only valid for extremely thin crystals.**

Fundamental equation

The fundamental equation of the scattering of an electron by a scalar potential $V(\vec{r})$:

$$(\widehat{\Delta} + k_0^2)|\Phi >= V(\vec{r})|\Phi >$$

The Dirac notation is used is this document[10]. Observing that the incidents electrons have a kinetic energy several orders of magnitude larger that the interaction energy, on can write (see figure page 19):

$$|\Phi >= e^{ik_z z}|\Psi >= e^{ik_z z} e^{i\pi\vec{\chi}\cdot\vec{\rho}}$$

The electron propagation is thus decomposed into 2 parts:

- A very fast movement along the z direction where the electron has an energy several orders of magnitude larger than the interaction potential.
- A movement in the (x, y) plane where the kinetic and potential energies are of comparable.

The following equation is obtained[11] under the elastic and small angle scattering approximations:

$$i\frac{d}{dz}|\Psi(z) >= \widehat{H}(z)|\Psi(z) >$$

It is similar to the time dependent Schrödinger equation where time t is replaced by z.

[10] The notation is provided on page 26.

[11] See development page 58.

Notation

- Vector in 3-D: $\vec{r} = \{\vec{\rho}, z\} = (x, y, z)$
- Vector in 2-D: $\vec{\rho} = (x, y)$
- Wave vector 3-D: $\vec{k} = \{\vec{\chi}, k_z\}$
- Momentum 2-D: $\vec{q}$
- Closure: $\sum |\vec{q} >< \vec{q}| = 1$
- Reciprocal lattice vector: $\vec{g}$ or $\vec{h}$
- Closure reciprocal basis: $\sum |\vec{g} >< \vec{g}| = 1$ or $\sum |\vec{h} >< \vec{h}| = 1$
- Operator: $\widehat{O} = \sum o_j |j >< j|$ where the o_j and $|j>$ are the eigenvalues[12] and eigenfunctions of $\widehat{O}$.
- Projector on state $|j>$: $|j >< j|$
- Plane wave of wave vector $\vec{k}$ (3-D): $\psi(\vec{r}) = e^{i\vec{k}\,.\,\vec{r}}$
- Plane wave of wave vector $\vec{q}$ (2-D): $\phi(\vec{\rho}) = e^{i\vec{q}\,.\,\vec{\rho}}$
- Transfer function[13] $T(\vec{q}, \Delta z)$: $T(\vec{q}, \Delta z) = e^{-i\,2\pi\left[\frac{C_s \lambda^3 (\vec{q}\cdot\vec{q})^2}{4} - \frac{\Delta z\, \lambda\, \vec{q}\cdot\vec{q}}{2}\right]}$

[12] Eigenvalues are real when operator is hermitic.

[13] Note that the defocus Δz is positive for underfocus.

Initial state and signs

Initial state $|\chi>$:

$$|\chi>= e^{i\pi\vec{\chi}\cdot\vec{\rho}}$$

Fourier transform (3-D):

$$<\vec{u}|\vec{k}>=\int_{-\infty}^{\infty} e^{-i\vec{u}\,.\,\vec{r}}\psi(\vec{r})d\vec{r}=\int_{-\infty}^{\infty} e^{-i\vec{u}\,.\,\vec{r}}e^{i\vec{k}\,.\,\vec{r}}d\vec{r}=\delta(\vec{k}-\vec{u})$$

Fourier transform (2-D):

$$<\vec{q}|\vec{q'}>=\int_{-\infty}^{\infty} e^{-i\vec{q}\,.\,\vec{\rho}}\psi(\vec{\rho})d\vec{\rho}=\int_{-\infty}^{\infty} e^{-i\vec{q}\,.\,\vec{\rho}}e^{i\vec{q'}\,.\,\vec{\rho}}d\vec{\rho}=\delta(\vec{q'}-\vec{q})$$

Structure factor $F_{\vec{h}}$ of a unit cell with N atoms at $\vec{x}_i$, Debye-Waller temperature factor $e^{-DW^i\frac{\vec{h}\cdot\vec{h}}{4}}$ and site occupancy Oc^i:

$$F_{\vec{h}}=\sum_{i=1}^{i=N} f_{\vec{h}}^{i}\, e^{-i\,2\pi\vec{h}\cdot\vec{x}_i}\, e^{-DW^i\frac{\vec{h}\cdot\vec{h}}{4}}\, Oc^i$$

Other functions and signs

Phase object function $O(\vec{\rho})$ with projected potential $V_p(\vec{\rho})$ (positive):

$$O(\vec{\rho}) = e^{i\,\sigma_e\,V_p(\vec{\rho})}$$

Weak phase object approximation $WPOA(\vec{\rho})$:

$$WPOA(\vec{\rho}) = 1 + i\,\sigma_e V_p(\vec{\rho})$$

Fresnel propagator $P(\vec{\rho}, z)$:

$$P(\vec{\rho}, z) = e^{i\,k_z \frac{\vec{\rho}\cdot\vec{\rho}}{2z}}$$

Evolution operator

It is a postulate of quantum mechanics that the temporal evolution of a system is given by:

$$|\Psi(t)>=\widehat{U}(t,t_0)|\Psi(t)>=\widehat{U}(t,t_1)\widehat{U}(t_1,0)|\Psi(t)> \quad t\geq t_1\geq t_0$$

$$\widehat{U}(t,t)=\widehat{1}$$

$$\widehat{U}(t_0,t)=\widehat{U}^{\dagger}(t,t_0)$$

In our case z replaces t and the evolution of the system from the initial state $|\Psi(0)>$ at z = 0 to the final state $|\Psi(z)>$ at z:

$$|\Psi(z)>=\widehat{U}(z,z_0)|\Psi(z)>$$

The evolution operator is the solution of:

$$i\frac{d}{dz}\widehat{U}(z,z_0)=\widehat{H}(z)\widehat{U}(z,z_0)$$

Where $\widehat{H}(z)$ is the hamiltonian of elastic diffraction:

$$\widehat{H}(z)=\frac{1}{2k_z}\left(\sum_q(q^2-\chi^2)|q><q|+\sum_{q,q'}|q><q|V(z)|q'><q'|\right)$$

Hamiltonian of elastic diffraction

$\widehat{H}(z)$ depends on the space variable (x, y) and z in the direction of propagation behaves like the time parameter of the Schrödinger equation.

The diagonal terms $(q^2 - \chi^2)\ \widehat{H}(z)$ are the deviations s_q from exact Bragg condition. They are calculated as[14]:

$$q^2 - \chi^2 = |\vec{\chi} + \vec{g}|^2 - \chi^2 = \chi^2 + 2\vec{\chi} \cdot \vec{g} + g^2 - \chi^2 = 2\vec{\chi} \cdot \vec{g} + g^2$$

The off-diagonal terms $< q|V(z)|q' >$ of $\widehat{H}(z)$ are the 2-D Fourier coefficients of the scattering potential.

As the diagonal terms increases quadratically with $|q|$, whereas the off-diagonal terms decrease to zero for large values of $|q|$, reciprocal nodes Q far away from the Ewald sphere do not contribute to diffraction. One can restrict the q basis to vectors such that q^2 is not too large compared to the maximum value of $< q|V(z)|q' >$.

[14] see figure page 19.

Diffraction: transition probability

Final state $|\Psi_z>$ of electron after interaction with potential $V(\vec{\rho}, z)$:

$$|\Psi_z> = \widehat{U}(z,0)|\Psi_0>$$

Transition probability from the initial state $|\chi>$ to the final state $|q>$, $\omega_{\chi \to q}(z,0)$, is the module square of $<q|\widehat{U}(z,0)|\chi>$ (intensity of beam diffracted to $|q>$).

Intensity diffracted to $|q>$:

$$\omega_{\chi \to q}(z,0) = |<q|\widehat{U}(z,0)|\chi>|^2$$

Intensity of diffracted beam $|q>$

The transition probability from $|\Psi(z_0)>$ or initial state $|\chi>$ to some final state $|q>$.

$$\omega_{\chi \rightarrow q}(z,0) = |<q|\widehat{U}(z,0)|\chi>|^2$$

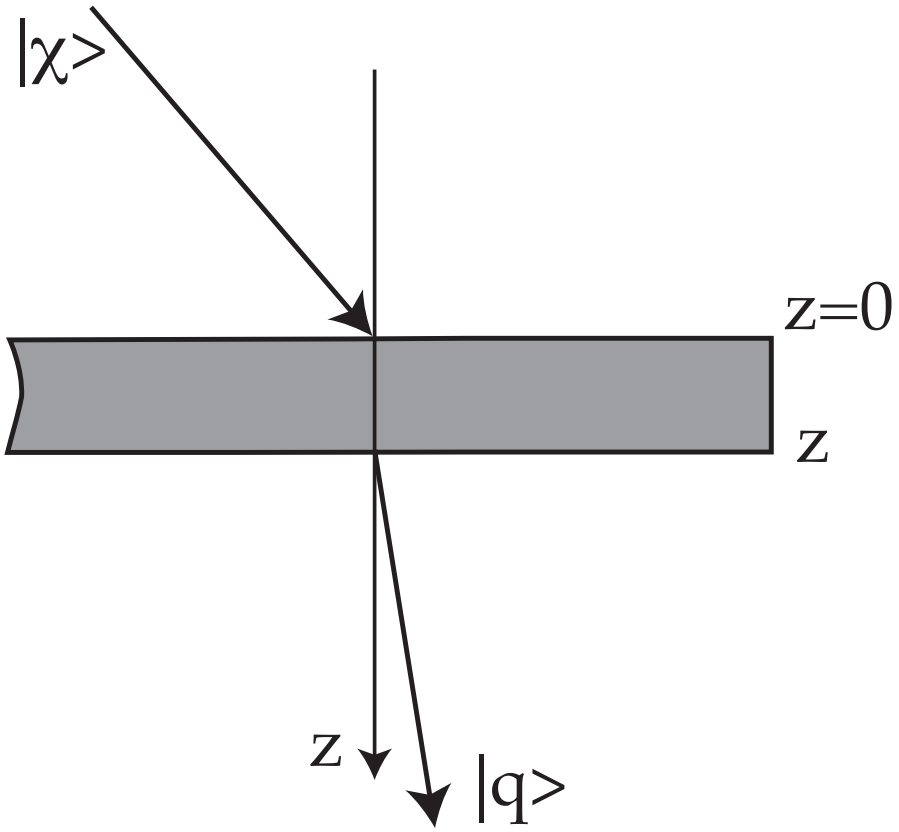

To calculate the intensity or transition probability $\omega_{\chi \rightarrow q}(z,0)$ we must calculate $\widehat{U}(z,0)$

Intensity of the wave function

Wave function intensity $\Psi(\rho; z)$ at exit face of crystal slab $\Longrightarrow$ transition probability from initial state $|\chi>$ to final state $|\rho>$:

$$\omega_o \rightarrow \rho(z,0) = |<\rho|\widehat{U}(z,0)|\chi>|^2$$

With a discrete set of $|q>$:

$$\omega_o \rightarrow \rho(z,0) = |\sum_q <\rho|q><q|\widehat{U}(z,0)|\chi>|^2$$

Where:

- $<q|\widehat{U}(z,0)|\chi>$ Fourier transform of object wave function.
- $\sum_q <\rho|q><q|\widehat{U}(z,0)|\chi>$ the Fourier synthesis of the image wave function.

Intensity in image plane

Intensity observed at point ρ in the image plane is modified by the transfer function of the microscope $T(q', q)$ that couples states $|q' >$ and $|q >$ (matrix $T(q', q)$).

Image intensity is given by:

$$\omega_o \rightarrow \rho(z, 0) = |\sum_q \sum_{q'} < \rho|q' >< q'|T(q', q)|q >< q|\widehat{U}(z, 0)|\chi >|^2$$

Fourier components of the wave function in image plane of objective lens are modified by $< q'|T(q', q)|q >$ (Abbe theory of image formation).

Abbe image formation: transfer function

The terms $\sum_{q'} < \rho | q^{'} >$ show that the wave function is obtained by inverse Fourier transform (Fourier synthesis).

In back focal plane of objective lens Fourier components of image wave function:

$$< q^{'} | T(q^{'}, q) | q >< q | \widehat{U}(z, 0) | \chi >$$

The microscope introduces a coupling between the diffracted beams when transferred by the objective lens.
When transfer is linear (for example in WPOA (weak phase object approximation) the transfer matrix $< q' | T(q', q) | q >$ is diagonal:

$$< q' | T(q', q) | q >= T(q) \delta(q' - q)$$

In this particularly simple case the image intensity is:

$$\omega_o \rightarrow \rho(z, 0) = | \sum_q < \rho | q > T(q) < q | \widehat{U}(z, 0) | \chi > |^2$$

HRTEM modeling

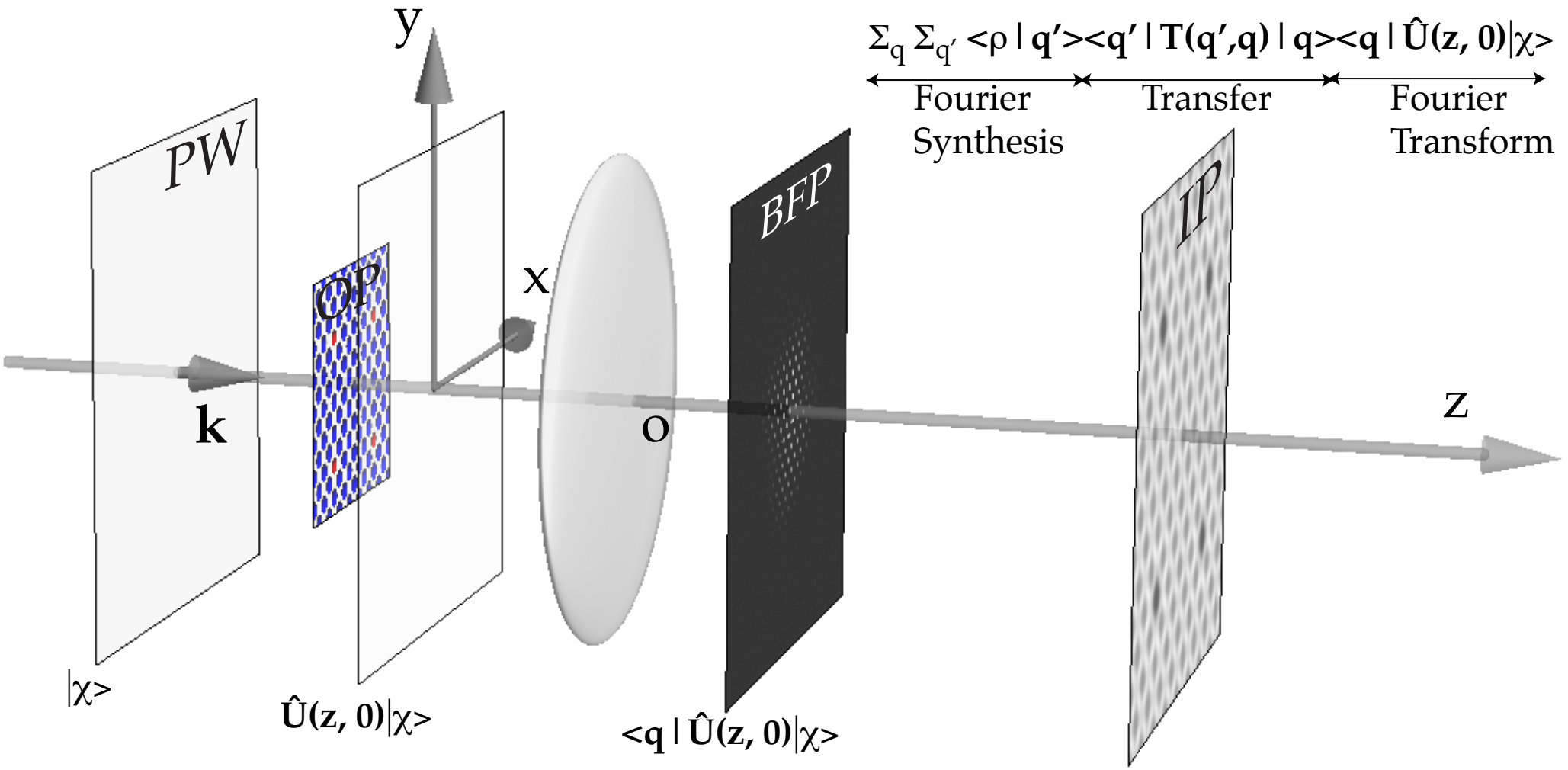

Some remarks

Finally, let us remark that the symmetry properties of the diffraction patterns and high resolution images are intrinsically tied to the properties of the transition probabilities $\omega_{o \to \rho}(z, 0)$ and $\omega_{\chi \to q}(z, 0)$.

Evolution operator $\widehat{U} \Longrightarrow$ key to understand not only symmetries, but also contrast of bright and dark field images of defects.

This systematic approach due to D. Gratias and R. Portier ([1]) unifies all the different methods of image simulation in transmission electron microscopy.

Approximations

$$H(z) = \frac{1}{2K}(-\nabla^2 - \chi^2 + V(z)) = H^0 + \frac{V(z)}{2K}$$

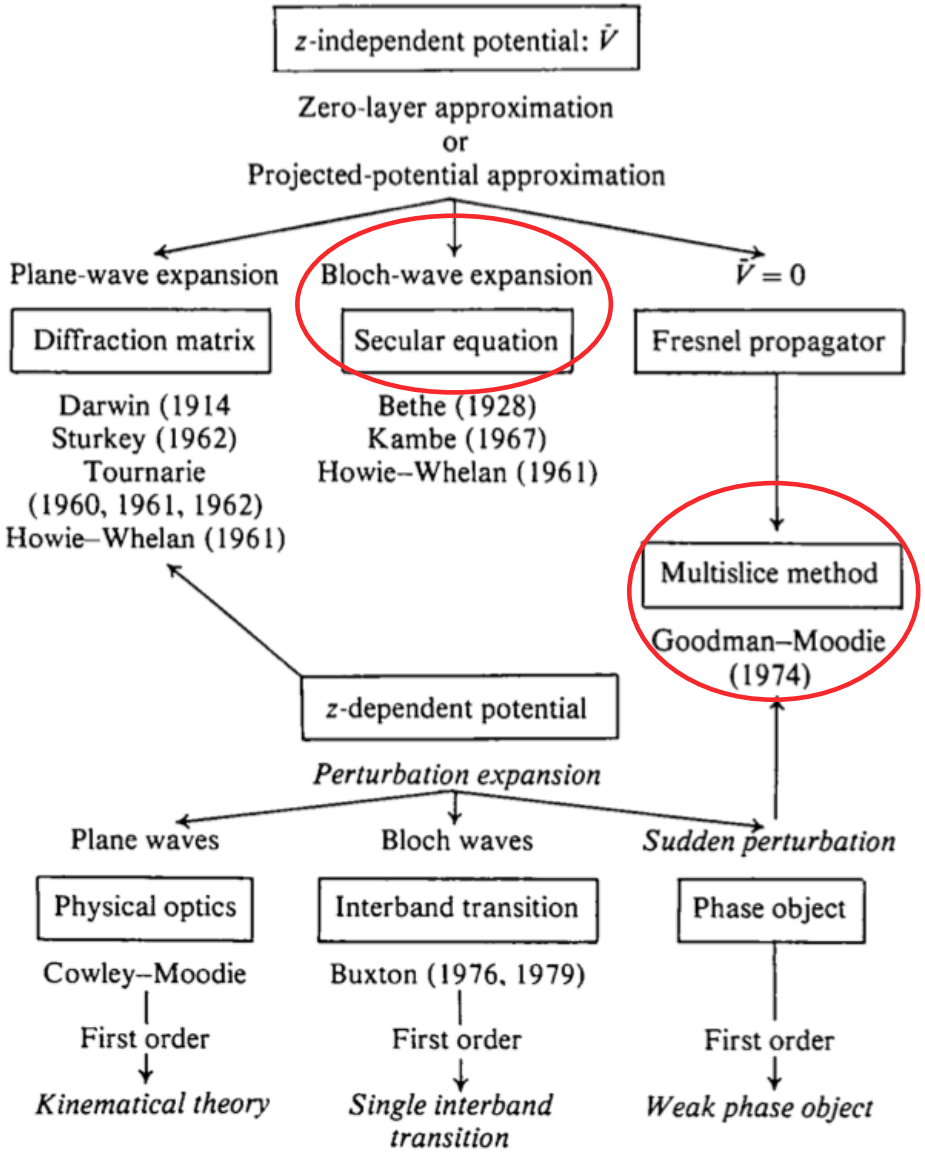

Figure: From Gratias and Portier [1]

Two approximations

All approximations are numerically equivalent, but perform best in particular cases.

We will consider only 2 approximations:

- The multislice approximation[15].
- The Blochwave method[16].

The multislice method performs best when simulating crystalline or amorphous solids of large unit cell or containing defects while the Bloch-wave method is adapted to the calculation of crystalline solids of small unit cell and in any [uvw] orientation. The Bloch-wave method has also several advantages (speed, ease of use) for simulating CBED, LACBED or PED patterns and for polarity and chirality determination.

[15] J. Cowley and A.F. Moodie, Proc. Phys. Soc. B70 (1957) 486, 497 and 505.

[16] H. A. Bethe, Ann. Phys. 87 (1928), 55.

Multislice method

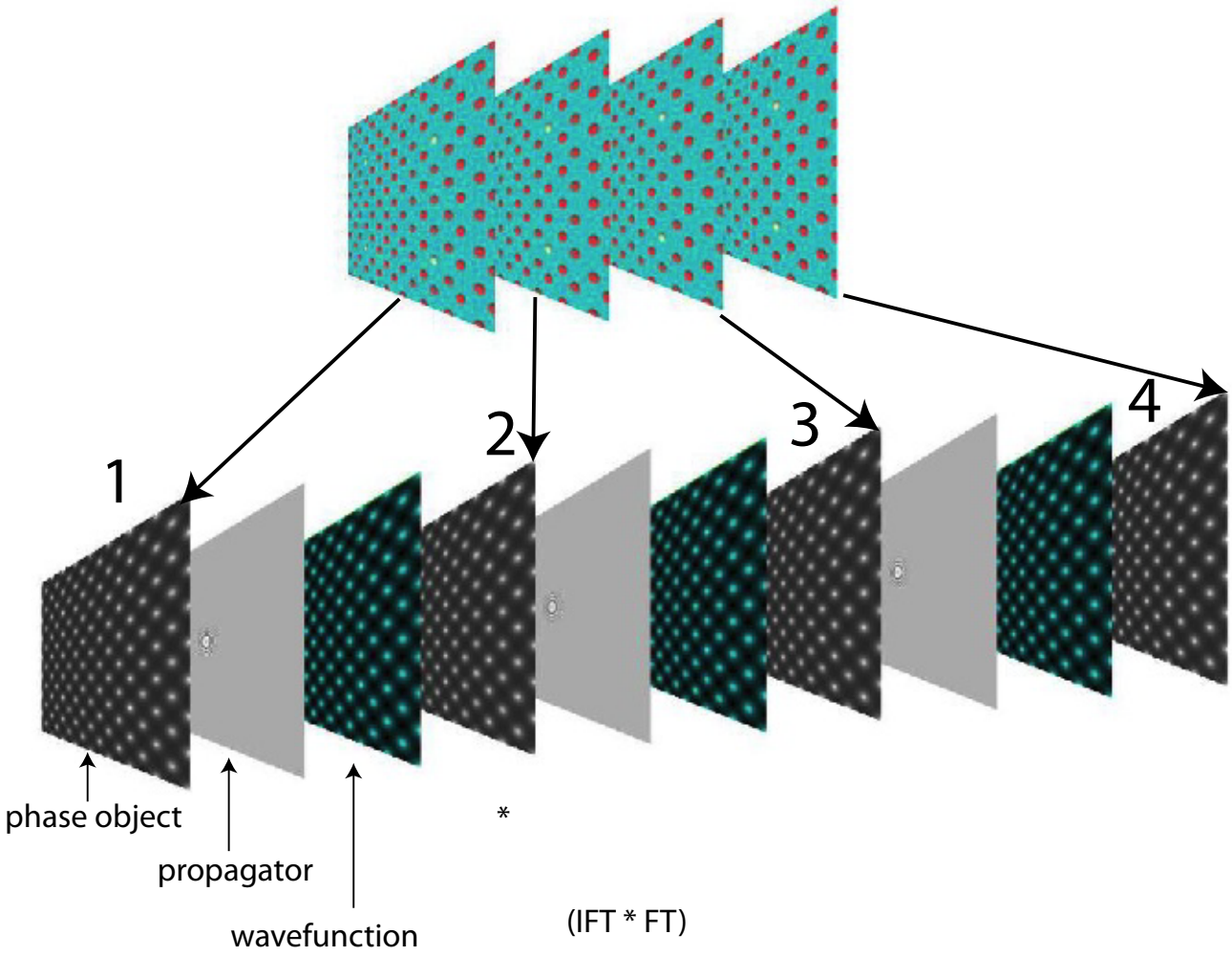

The solid is sliced into thin sub-slices. The incident wave-function is transfered by the first slice (diffraction) and propagated to the next one. The propagation is done within the Fresnel approximation, the distance between the slices being 20 - 50 times the wavelength[17].

[17] file://localhost/Users/pierrestadelmann/Desktop/HamiltonJune2012/html/PtOct/b.html

Multislice algorithm

- Diffractor: transfer by a slice $\Rightarrow$ multiplication by phase object function ($POF(\vec{\rho})$).
- Propagator: propagation between slices $\Rightarrow$ convolution by the Fresnel propagator (is nowadays performed by FFT followed by a multiplication and an inverse FFT (FT^{-1}, multiplication, FFT)).

Diffractor

When only the potential term is conserved in the hamiltonian:

$$\widehat{H}^d = \frac{1}{2k_z} V(\rho, z)$$

$\widehat{H}^d$ is diagonal on $|\rho>$.

$$\widehat{H}^d|\rho> = \frac{1}{2k_z} V(\rho, z)|\rho>$$

The evolution operator is then given by:

$$\widehat{U}^d(z, 0) = e^{-\frac{i}{2k_z}\int_0^z V(\rho,\tau)d\tau}$$

The wave-function at thickness z is written as:

$$\Psi(z) = \widehat{U}^d(z, 0)|0> = e^{-\frac{i}{2k_z}\int_0^z V(\rho,\tau)d\tau}|0>$$

$po(\rho) = \widehat{U}^d(z, 0)$ is the phase object (PO). The weak phase object approximation (WPOA) develops PO is Taylor series. Note that in the above equation the projected potential (energy term) is negative (scattering potential times the electron charge).

Propagator

When the potential can be neglected (vacuum propagation), the hamiltonian reduces to:

$$\widehat{H}^0 = -\frac{1}{2k_z}\left[\widehat{\Delta} + \chi^2\right]$$

It diagonal on $|q>$:

$$\widehat{H}^0|q> = \frac{q^2 - \chi^2}{2k_z}|q>$$

The evolution operator is then given by:

$$\widehat{U}^0(z,0) = e^{-i\widehat{H}^0 z} = \int e^{-i\frac{q^2-\chi^2}{2k_z}z}|q><q|d^2q$$

In $|\rho>$ representation, propagation from point ρ_1 of the entrance face to point ρ_2 of the exit face of the crystal slab is:

$$<\rho_2|\widehat{U}^0(z,0)|\rho_1> = \int e^{-i\frac{q^2-\chi^2}{2k_z}z} <\rho_2|q><q|\rho_1> d^2q$$

$$<q|\rho_1> = e^{-iq\rho_2}$$

$$<\rho_2|q> = e^{iq\rho_2}$$

$$\widehat{U}^0(z,0) = e^{-i\frac{k_z(\rho_2-\rho_1)^2}{2z}}$$

Example: Pt catalyst

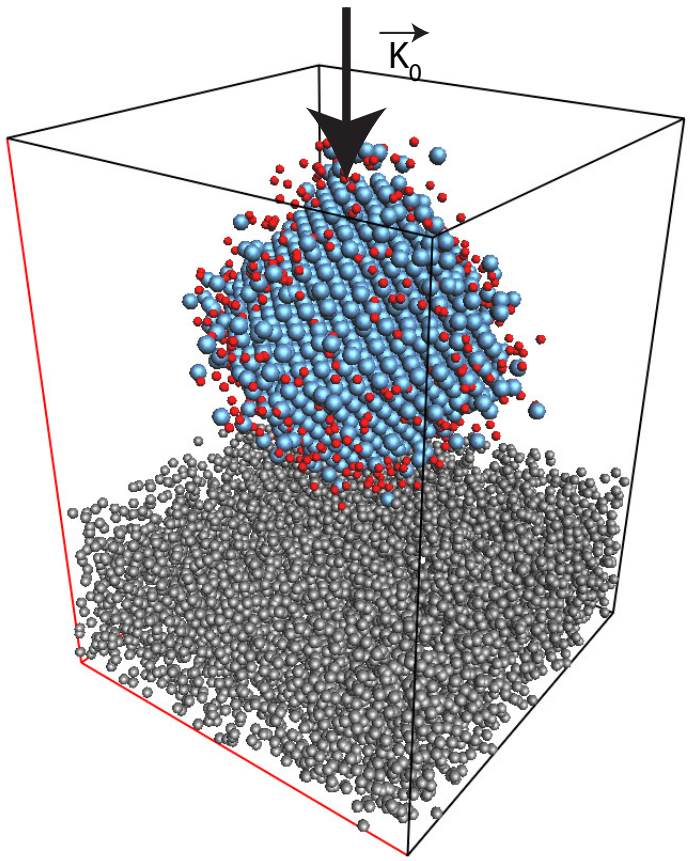

A

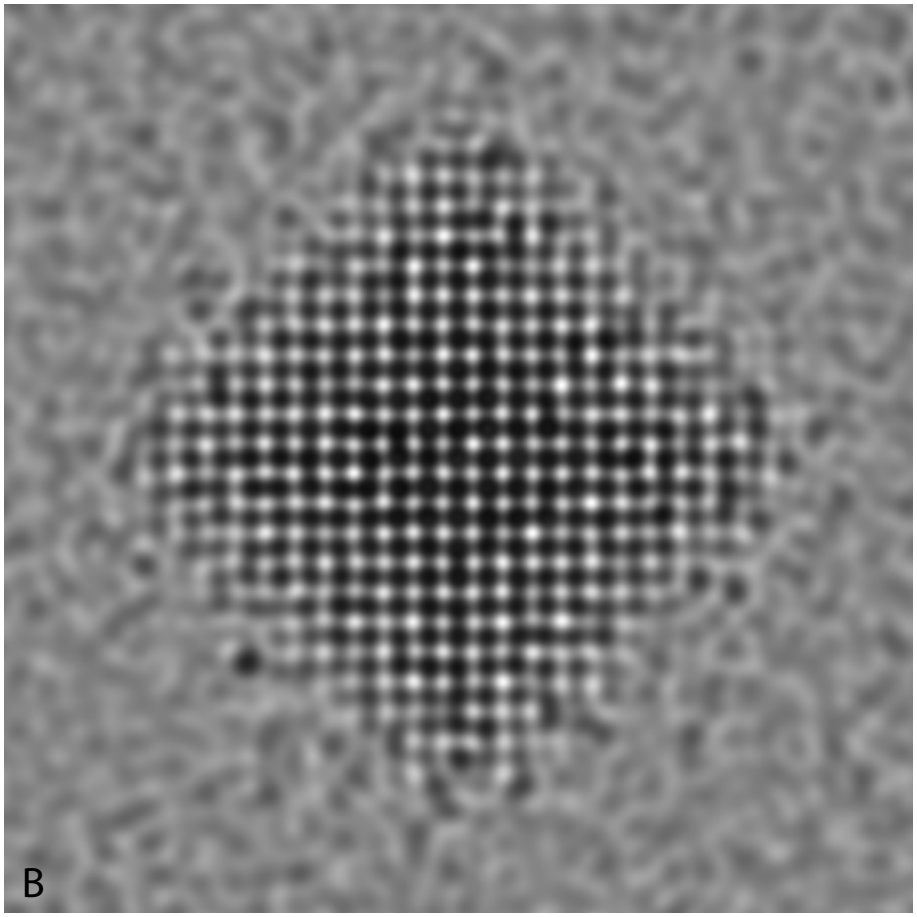

B

A: catalyst model (9500 atoms)[18]*. B: HREM image (Jeol 400kV).*

[18] file://localhost/Users/pierrestadelmann/Desktop/HamiltonJune2012/html/pot3D/pot3D.html

Example multislice: Fe_3S_4

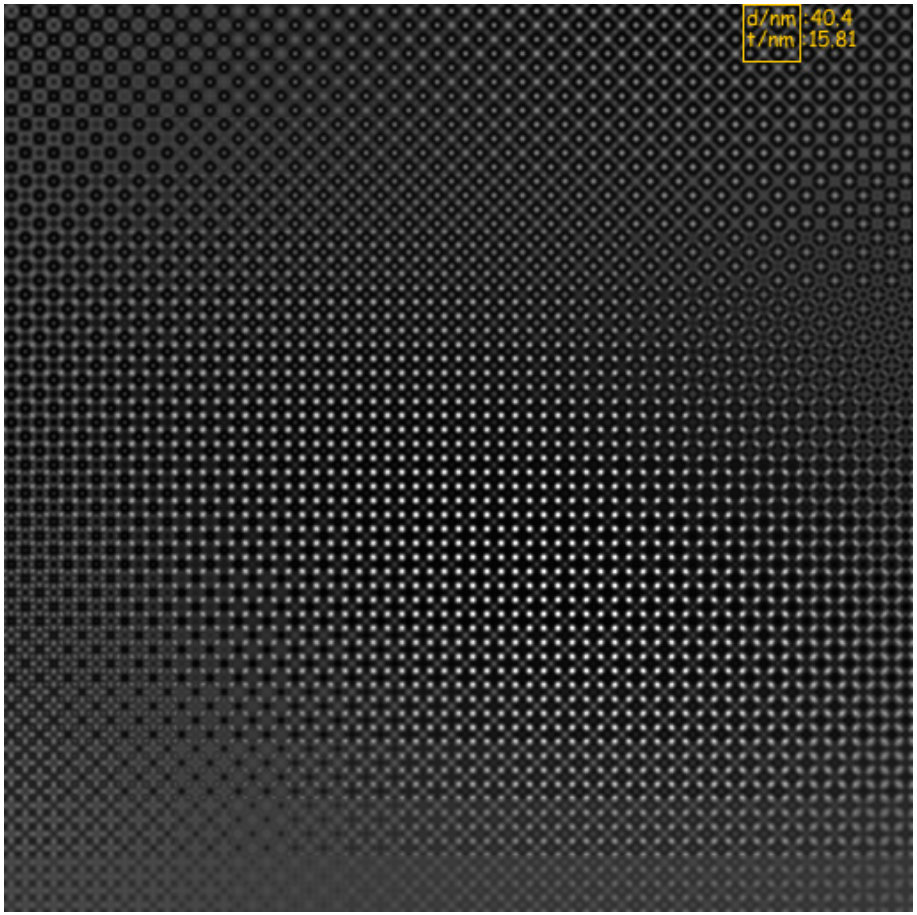

Figure: Fe_3S_4 HREM map.

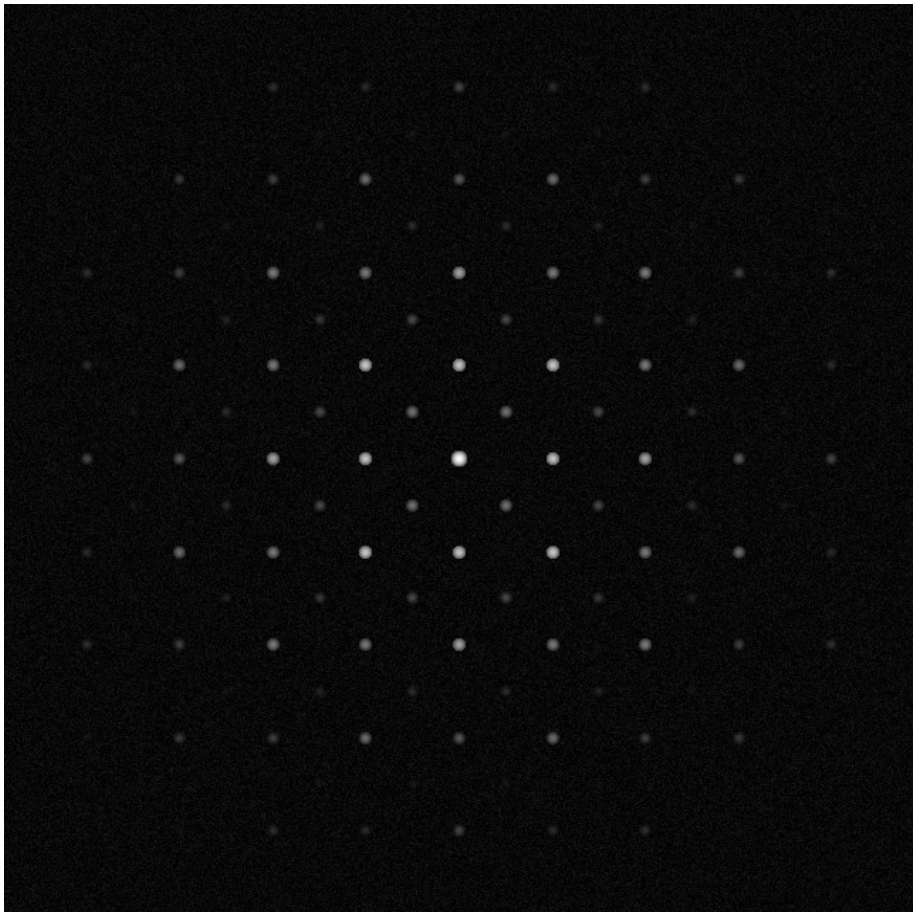

Figure: Fe_3S_4 SAED pattern.

Bloch wave method

When the scattering potential is periodic, the eigenstates $|j>$ of the propagating electrons are Bloch waves. The hamiltonian of the system is projected on the eigenstates $|j>$ with eigenvalues γ_j (*"anpassung"* parameter).

$$\widehat{H} = \sum e^{-i\gamma_j} |j><j|$$

The evolution operator is then given by:

$$\widehat{U}(z,0) = \sum_j e^{-i\gamma_j z} |j><j|$$

The wave-function at z developed on plane waves basis $|q>$:

$$\Psi(z) = \sum_q \phi_q(z)|q>$$

$$\phi_q(z) = <q|\widehat{U}(z,0)|0> = \sum_j e^{-i\gamma_j z} <q|j><j|0>$$

$$c_0^{*j} = <j|0> \text{ and } c_q^j = <q|j>$$

where in usual notation c_0^{*j} and c_q^j are the Bloch-wave excitations (component of the initial state $|0>$ on $|j>$) and coefficients (component of reflection $|q>$ on $|j>$) respectively.

Bloch wave coefficients c_0^{*j} and c_q^j

The Bloch wave coefficients c_0^{*j} and c_q^j are determined from:

$$\widehat{H}|j>=\gamma_j|j> \Rightarrow <q|\widehat{H}|j>=\gamma_j<q|j>$$

$$<q|\frac{1}{2k_z}(-\widehat{\Delta}-\chi^2+\overline{V})|j>=\gamma_j<q|j>$$

$$\frac{q^2-\chi^2}{2k_z}<q|j>+\sum_{q'}<q|\frac{\overline{V}}{2k_z}|q'><q'|j>=\gamma_j<q|j>$$

$$\frac{q^2-\chi^2}{2k_z}c_q^j+\frac{V_{q'-q}}{2k_z}c_{q'}^j=\gamma_j c_q^j$$

It is transformed in an homogenous system (in matrix form):

$$\left[\left[\frac{g^2-\chi^2}{2k_z}-\lambda\widehat{I}+\frac{\overline{V}_{h-g}}{2k_z}\right]\right][c]=0$$

The eigenvalues γ_j and eigenvectors $[c]$ are determined for a limited set of plane wave $|g_i>$. In practice, the set dimension is increased until the eigenvalues converge. The Bloch waves are finally given by:

$$|j^{(n)}>=\sum_i c_i^n|g_i>$$

The Bloch waves (eigenstates) propagate independently in the crystal.

Example: ZnTe [110]

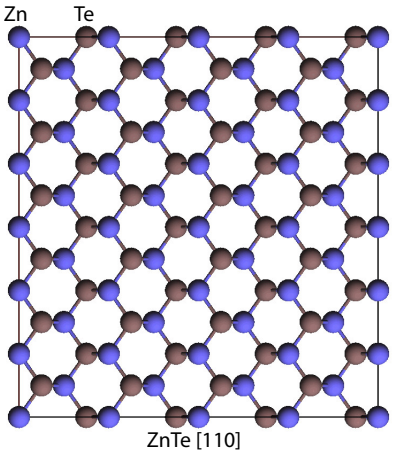

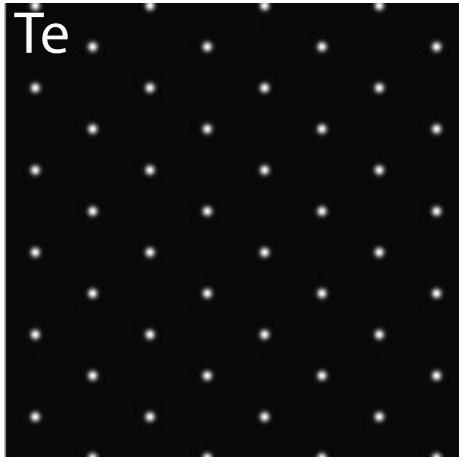

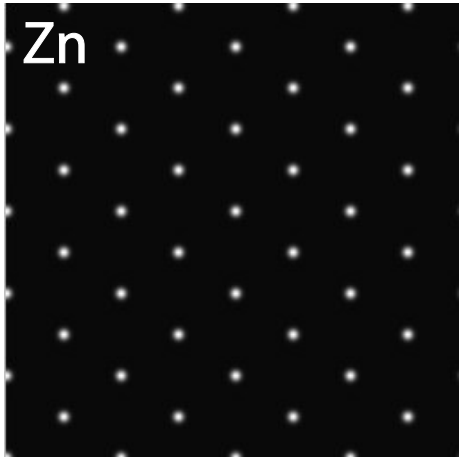

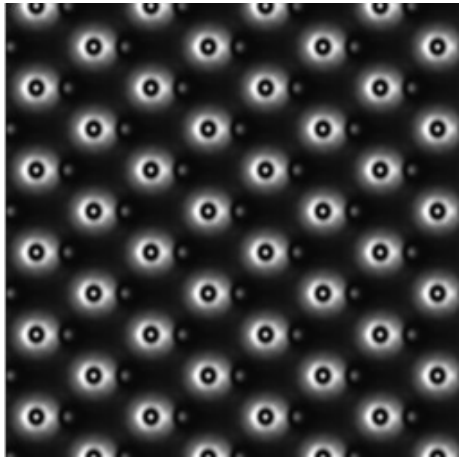

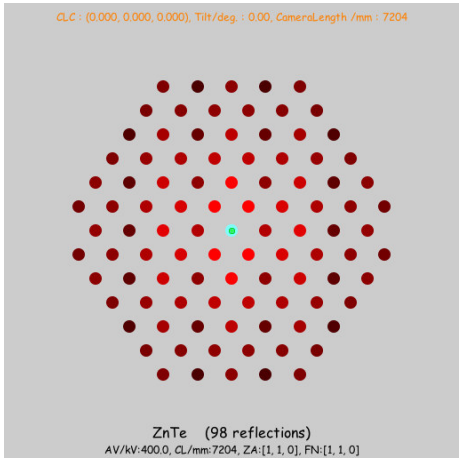

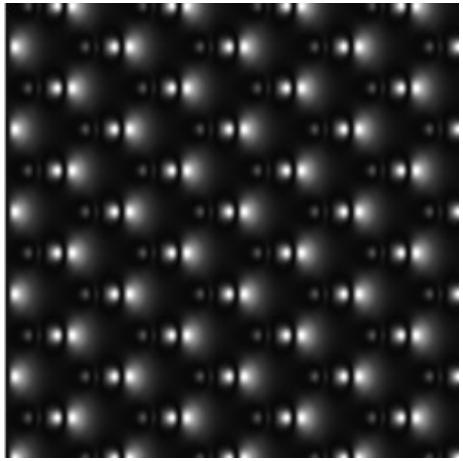

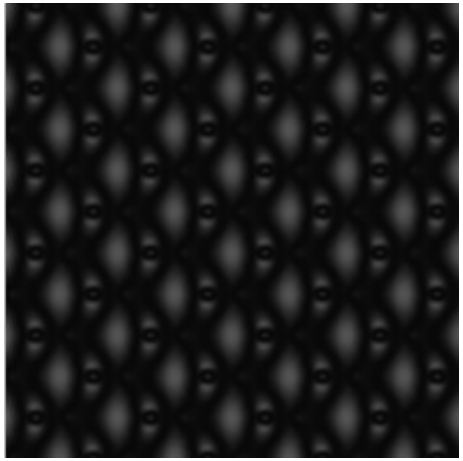

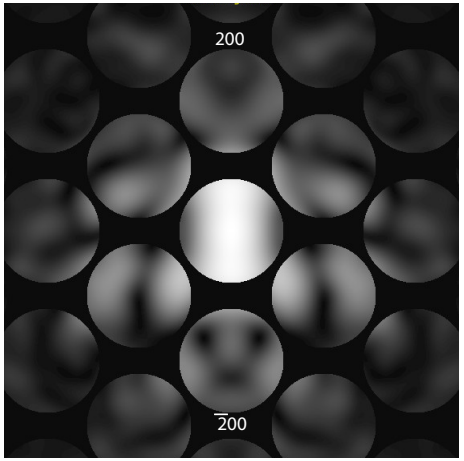

1 + 49 reflections. Only 5 Bloch-waves are excited when $|\chi >= 0$.

Bloch-wave example: LACBED - specimen thickness

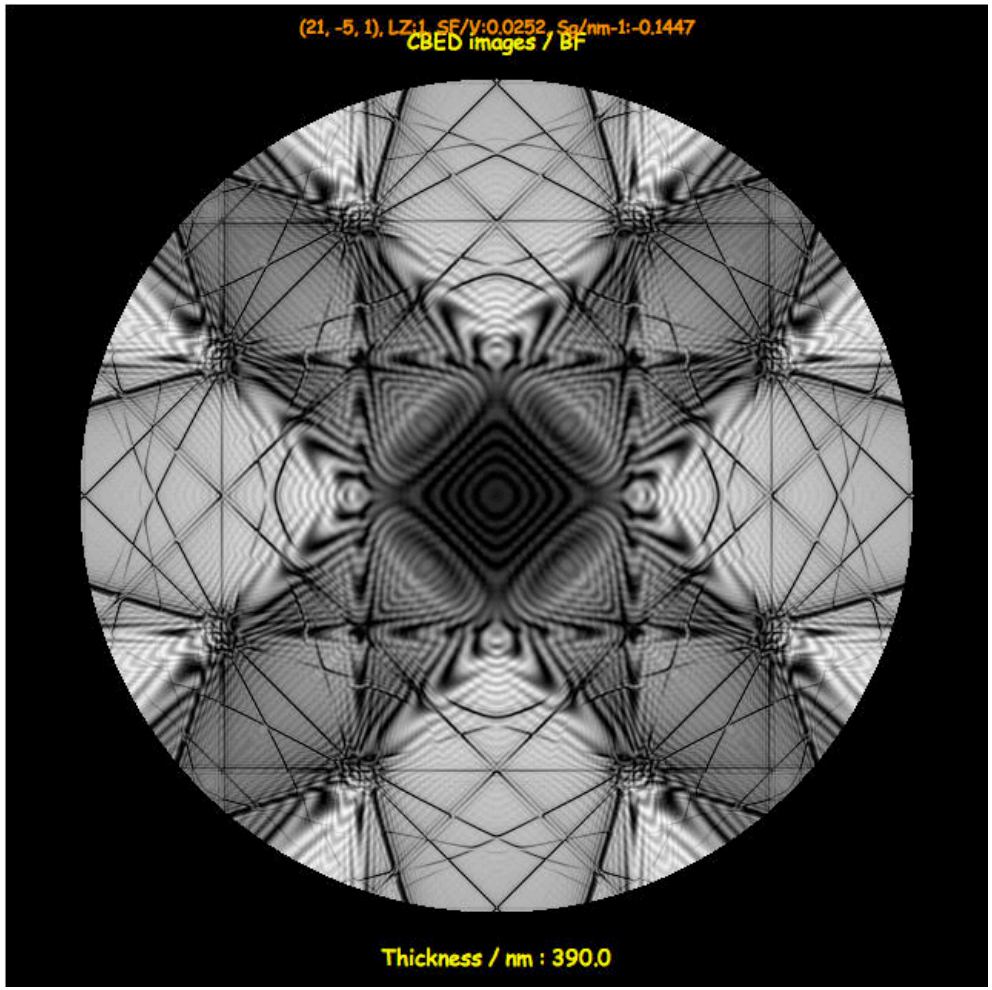

Figure: Simulation.

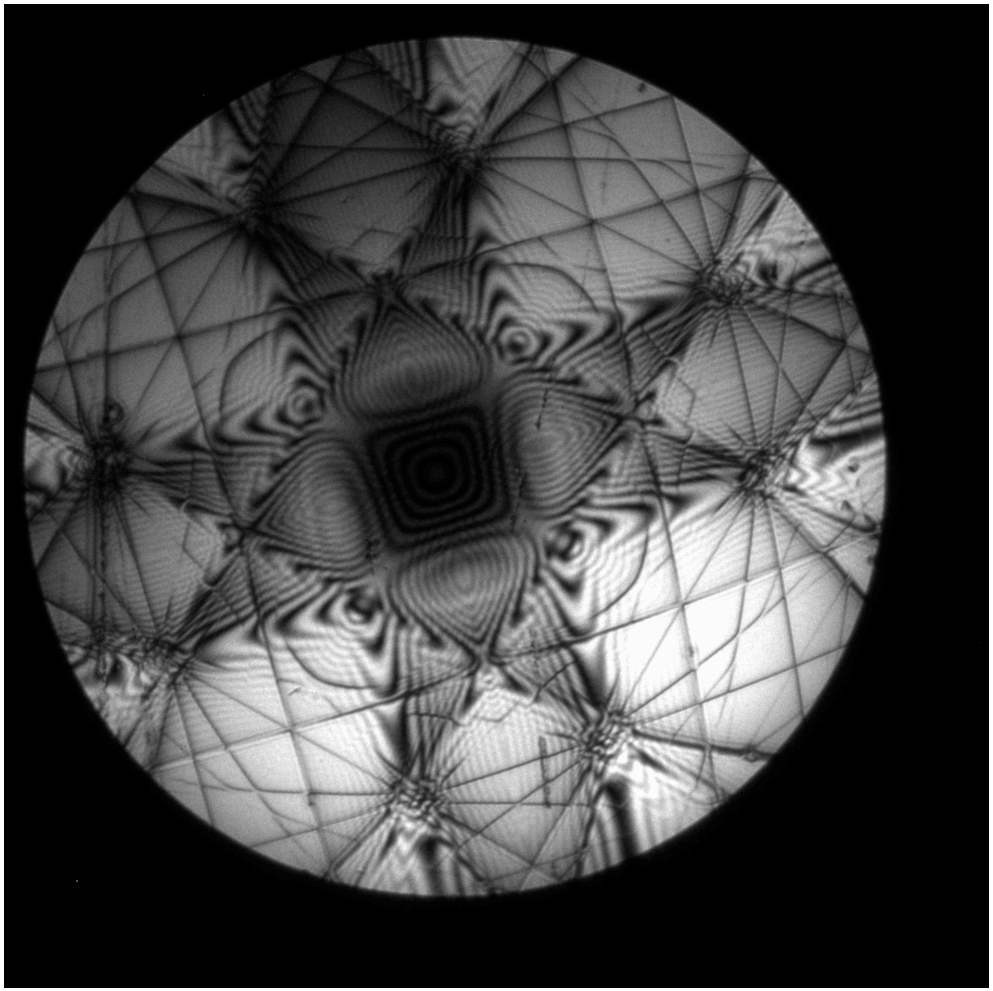

Figure: Web site EM centre - Monash university (J. Etheridge).

Bloch-wave simulation of LACBED pattern[19].

[19] file://localhost/Users/pierrestadelmann/Desktop/HamiltonJune2012/html/Si001/Si001.html

Bloch-wave example: ZnO polarity

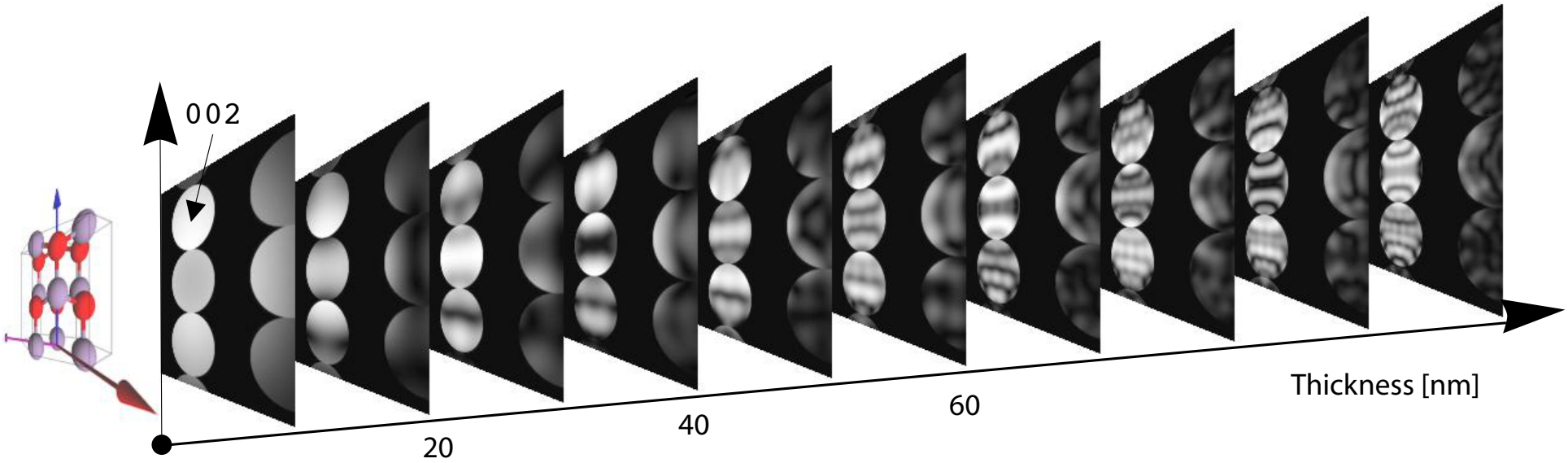

(200) and ($\bar{2}$00) CBED disks show different intensity pattern ($F_{200} = 10.86$ V, $F_{\bar{2}00} = 10.71$ V)[20].

[20] file://localhost/Users/pierrestadelmann/Desktop/HamiltonJune2012/Crystals/ZnO/ZnO.html

Example: Fe_3S_4

Figure: Fe_3S_4 HREM map Bloch-wave method (1 + 436 BW)

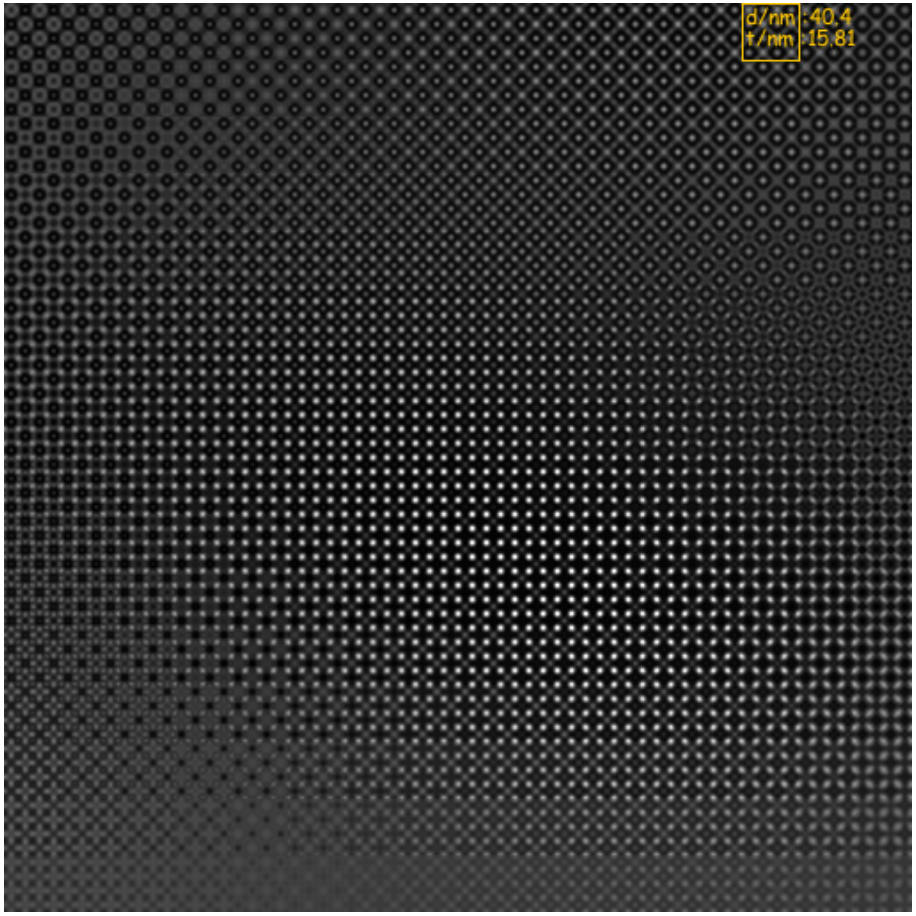

Figure: Fe_3S_4 HREM map multislice method (256x256).

Detector MTF: Gatan 1K x 1K CCD

To make quantitative comparison with experimental HRTEM images the MTF of the detector must be introduced in the simulation.

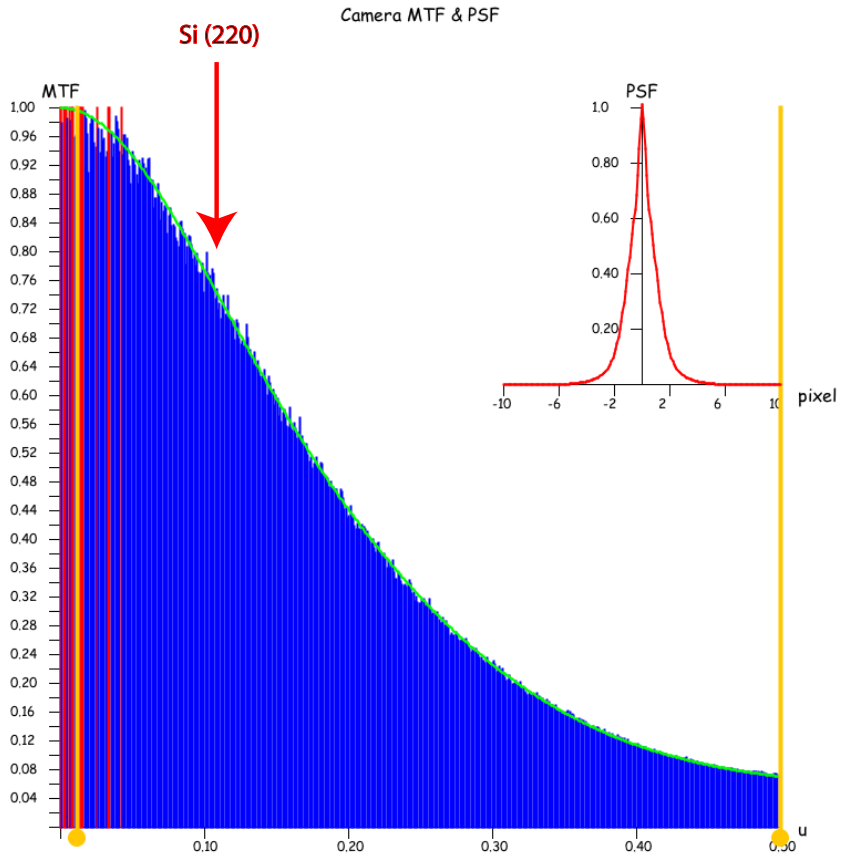

Figure: At high magnification Si (220) planes imaged with high contrast.

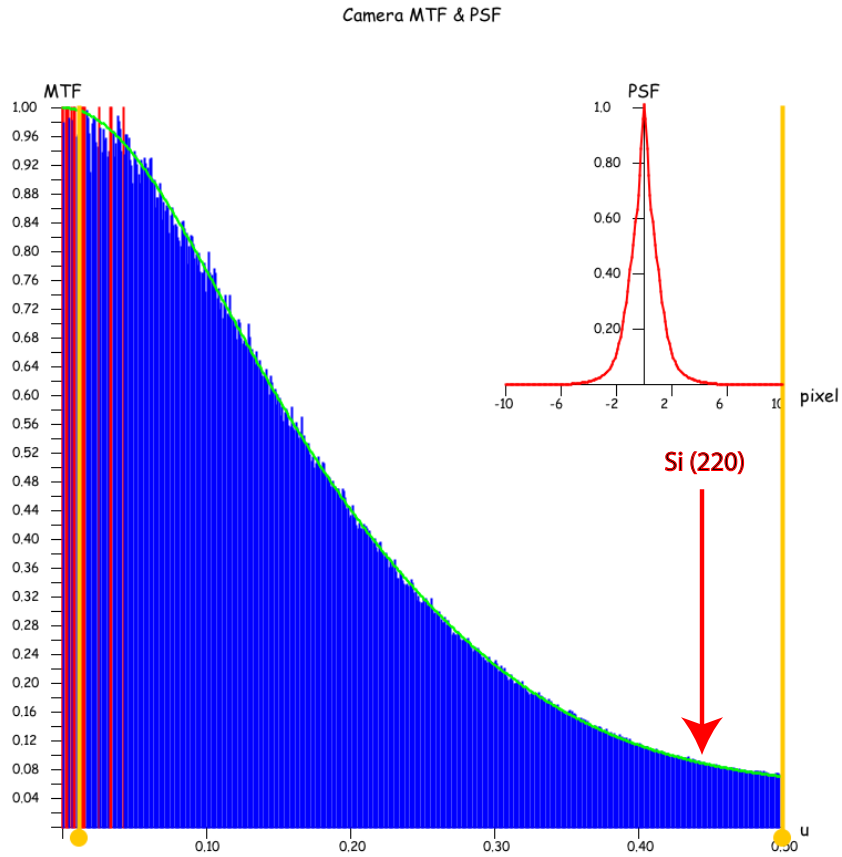

Figure: At low magnification Si (220) planes imaged with low contrast.

For quantitative comparison always use highest magnification!

CCD MTF: high magnification

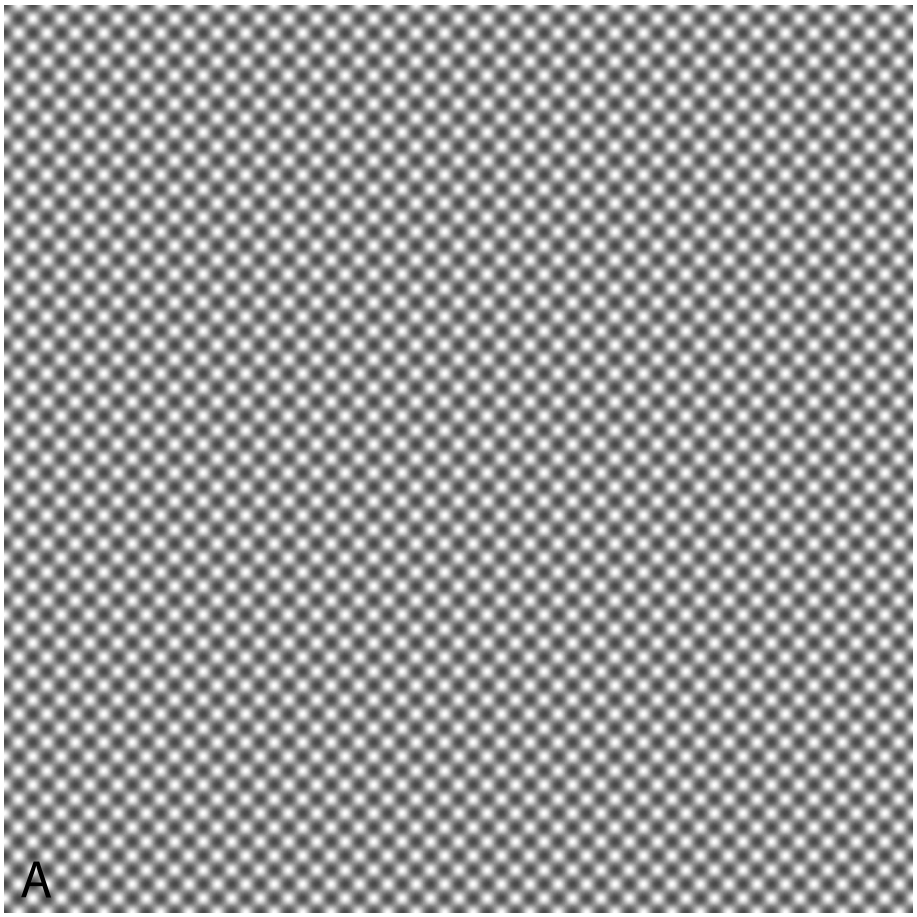

Figure: A: Si [001] simulation.

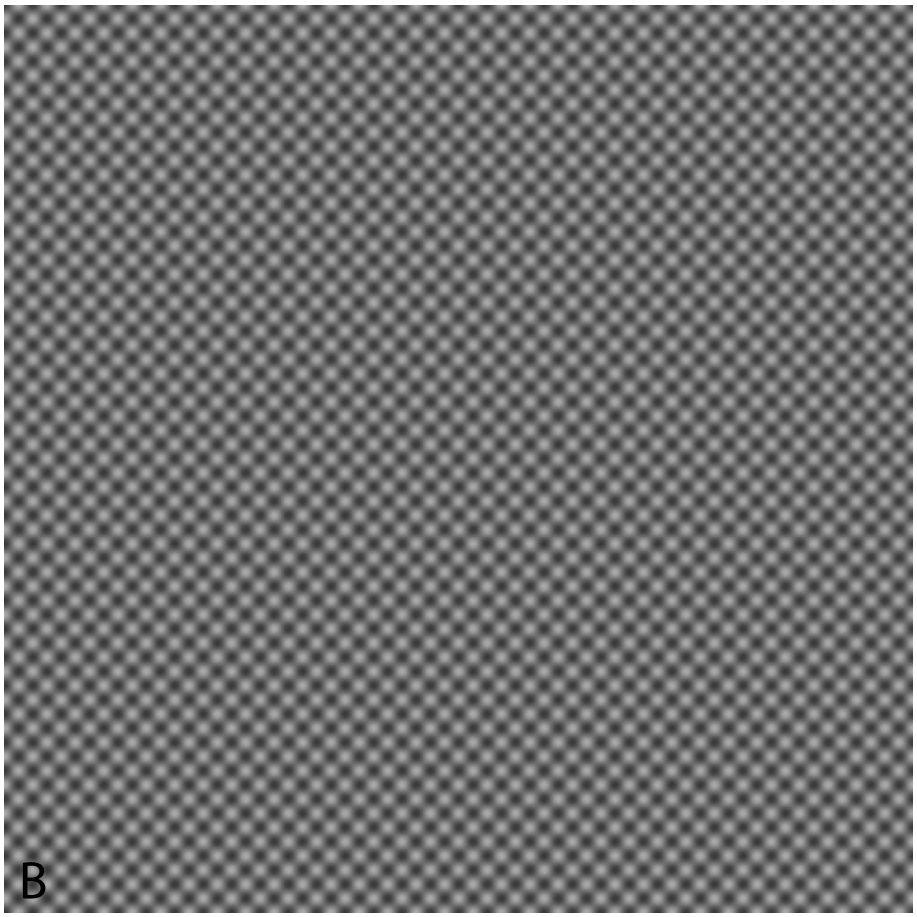

Figure: B: Si [001], simulation + CCD MTF.

CCD MTF: low magnification

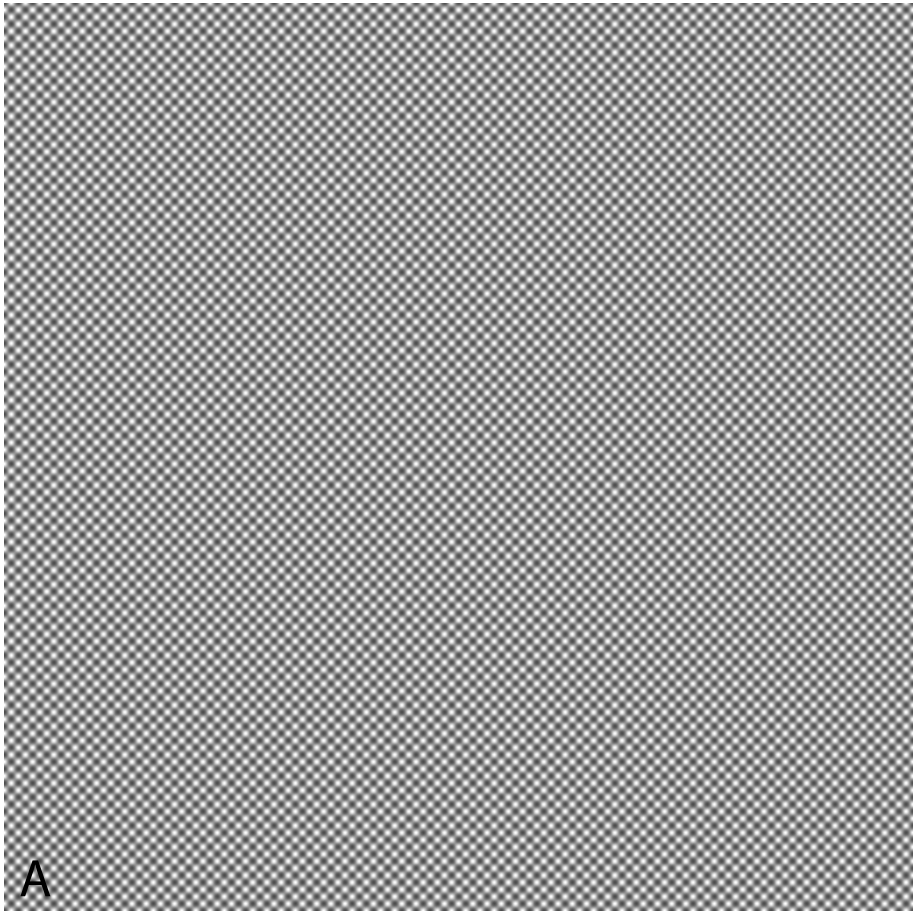

Figure: A: Si [001] simulation.

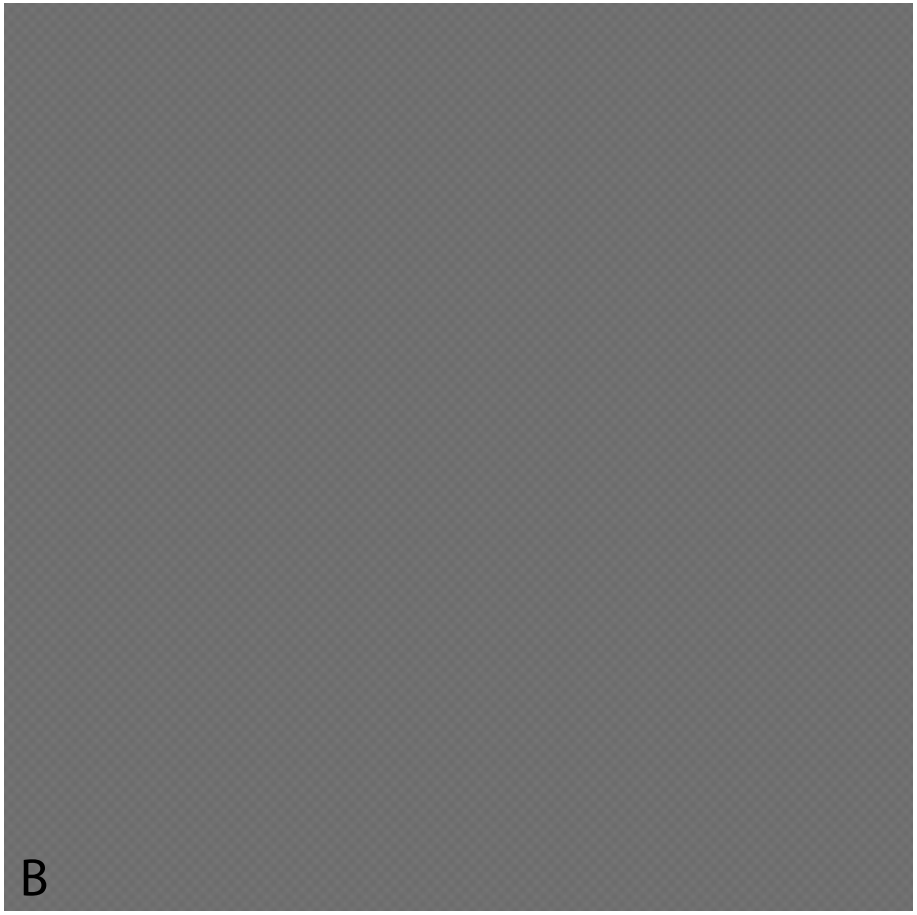

Figure: B: Si [001], simulation + CCD MTF.

Future of HRTEM simulation with the C_s and C_c correction?

Example: CdCu_2, visibility of the 3 Cu atomic columns.

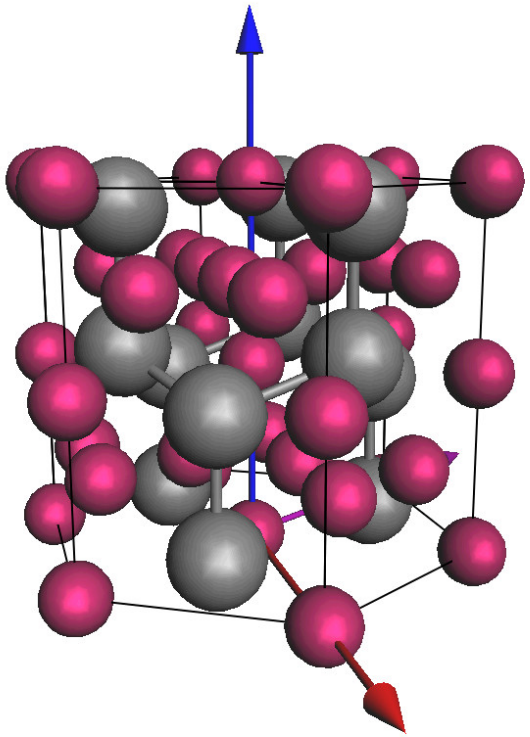

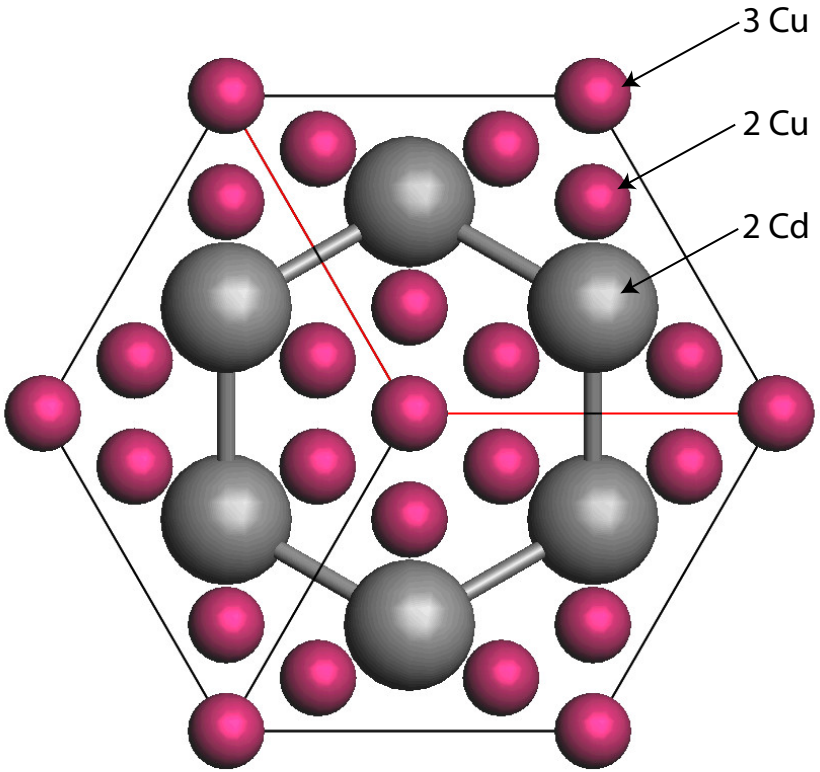

HRTEM image simulation conditions

Acc. [kV]	$C_s[mm]$	$C_5[mm]$	$C_c[mm]$	$\Delta E[eV]$	Z [nm]	$\Delta z[nm]$
300	-0.008	30	0.5	0.6	-4.9	1
300	-0.008	30	0.1	0.2	-2.0	1

Dynamical scattering effects are not affected by C_s and/or C_c corrected TEM!

$CdCu_2[001]$: imaging parameters set 1

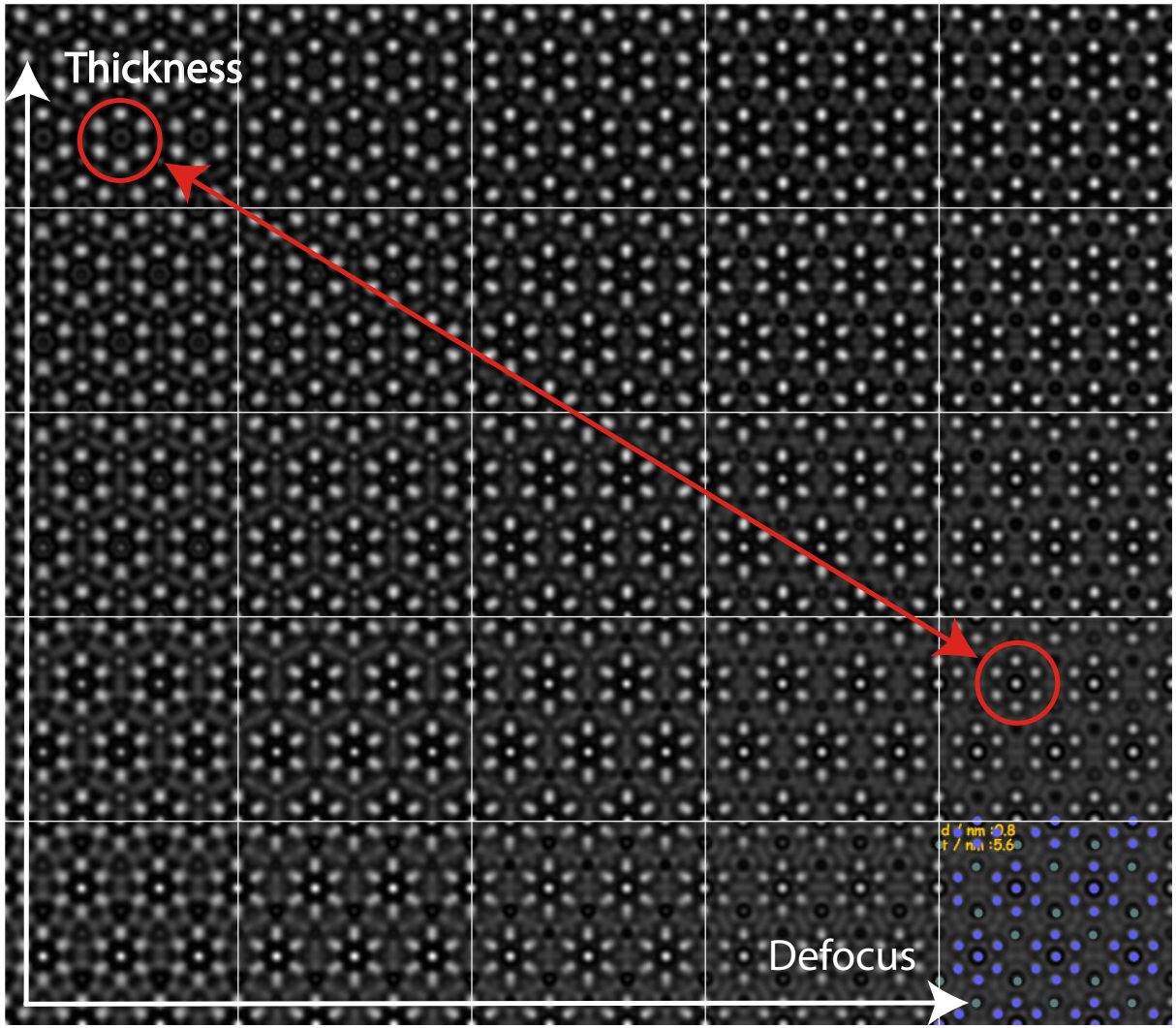

Visibility of 3 Cu atomic columns depends on specimen thickness and defocus.

$CdCu_2[001]$: imaging parameters set 2

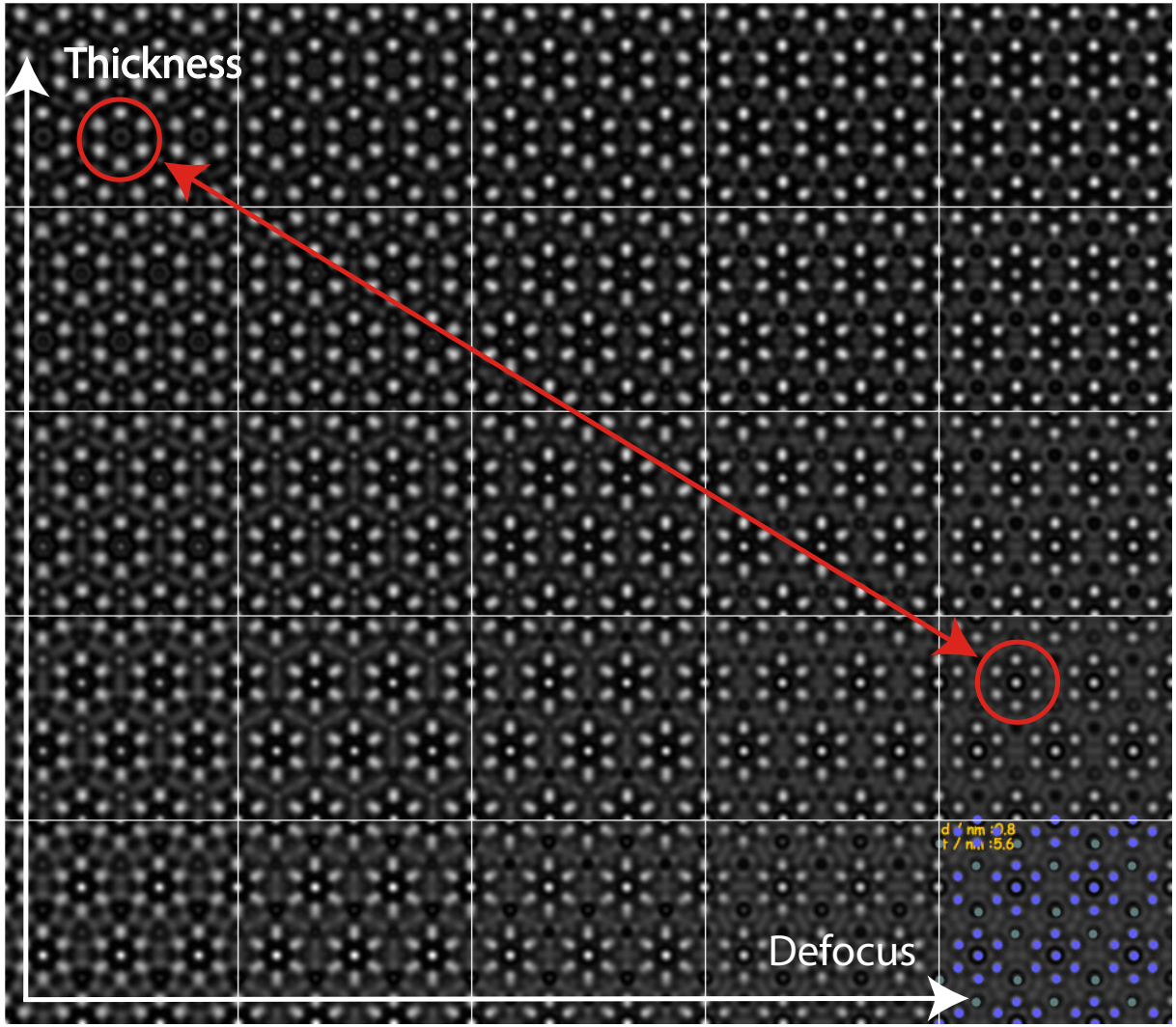

Improving C_c and ΔE does not affect the visibility of 3 the Cu atomic columns depends on specimen thickness and defocus.

Visibility of the 3 Cu atomic columns is affected dynamical scattering (1 MeV C_s and C_c TEM).

Dynamical theory of elastic scattering of high energy electron

We aim to understand in details multiple elastic scattering of electrons by crystals.

- High energy electron (eE).
- Periodic interaction potential $V(\vec{r})$.
- Time independent flux of incident electrons.

The fundamental equation of electron elastic scattering by a potential $V_v\,[Volt]$(positive inside a crystal) in the approximation of a stationary flux of electrons of a given energy $e\,E$ is the Schrödinger equation ([2]):

$$\triangle\Phi(\vec{r}) + \frac{2me}{\hbar^2}[E + V_v(\vec{r})]\Phi(\vec{r}) = 0$$

With a change of notation its is written as:

$$[\triangle + 4\pi^2 K_i^2]\ \Phi(\vec{r}) = -4\pi^2 V_v(\vec{r})\ \Phi(\vec{r})$$

Where the wavevector $|\vec{K}_i|$ of the incident electrons is given by:

$$|K_i| = \frac{\sqrt{2meE}}{h}$$

and

$$m = \gamma\ m_0$$

Schrödinger equation

The Laplacian $\triangle = \frac{\partial^2}{\partial x^2} + \frac{\partial^2}{\partial y^2} + \frac{\partial^2}{\partial z^2}$ is written as: $\triangle_\rho + \frac{\partial^2}{\partial z^2}$. As a result, $[\triangle + ...]e^{2\pi\imath k_z z}\Psi(\rho; z)$ is given by: $[\triangle_\rho + \frac{\partial^2}{\partial z^2} + ...]e^{2\pi\imath k_z z}\Psi(\rho; z)$.
Performing the z-differentiation:

$$\frac{\partial^2}{\partial z^2}e^{2\pi\imath k_z z}\Psi(\rho; z) = e^{2\pi\imath k_z z}[-4\pi^2 k_z^2 + 4\pi\imath k_z\frac{\partial}{\partial z} + \frac{\partial^2}{\partial z^2}]\Psi(\rho; z)$$

Inserting the last expression and dropping the term $e^{2\pi\imath k_z z}$:

$$[\triangle_\rho + 4\pi^2(K_i^2 - k_z^2 + V(\rho; z)) + 4\pi\imath k_z\frac{\partial}{\partial z} + \frac{\partial^2}{\partial z^2}]\Psi(\rho; z) = 0$$

Since $K_i^2 = k_z^2 + \chi^2$:

$$[\triangle_\rho + 4\pi^2\chi^2 + 4\pi^2 V(\rho; z) + 4\pi\imath k_z\frac{\partial}{\partial z} + \frac{\partial^2}{\partial z^2}]\Psi(\rho; z) = 0$$

Rearranging the last equation:

$$\imath\frac{\partial\Psi(\rho; z)}{\partial z} = -\frac{1}{4\pi k_z}[\triangle_\rho + 4\pi^2\chi^2 + 4\pi^2 V(\rho; z) + \frac{\partial^2}{\partial z^2}]\Psi(\rho; z)$$

Fundamental equation

$$\imath\frac{\partial\Psi(\rho;z)}{\partial z} = -\frac{1}{4\pi k_z}[\triangle_\rho + 4\pi^2\chi^2 + 4\pi^2 V(\rho;z) + \frac{\partial^2}{\partial z^2}]\Psi(\rho;z)$$

The term $|\frac{\partial^2\Psi(\rho;z)}{\partial z^2}|$ being much smaller than $|k_z\frac{\partial\Psi(\rho;z)}{\partial z}|$ we drop it (this is equivalent to neglect backscattering).

Fundamental equation of elastic scattering of high energy mono-kinetic electrons with a potential within the approximation of small angle scattering:

$$\imath\frac{\partial}{\partial z}\Psi(\rho;z) = -\frac{1}{4\pi k_z}[\triangle_\rho + 4\pi^2\chi^2 + 4\pi^2 V(\rho;z)]\Psi(\rho;z)$$

Time dependent Schrödinger equation $\Longrightarrow$ solution by many methods of quantum mechanics!

Remarks

- The approximations of the fundamental equation are equivalent to assume that the scattering potential is small compared to the accelerating potential and that k_z varies only slightly with z. It is in fact a quite good approximation, since the mean crystal potential is of the order of $10 - 20\ V$.
- Electron backscattering is neglected, the electron are moving forwards.
- The fundamental equation is actually equivalent to a 2-dimensional Schrödinger equation ($\rho = \{x, y\}$) where z plays the role of time. The system evolution is causal, from the past to the future.

Fundamental equation in Hamiltonian form:

$$\imath \frac{\partial}{\partial z} \Psi = H\ \psi$$

where:

$$H = -\frac{1}{4\pi k_z}[\triangle_\rho + 4\pi^2\chi^2 + 4\pi^2 V(\rho; z)] = H_o + \frac{4\pi^2 V(\rho; z)}{4\pi k_z}$$

A fundamental postulate of quantum mechanics ([3, 4]) says that the evolution operator obeys the equation:

$$\imath \frac{\partial}{\partial z} U(z, 0) = H(\rho; z)\ U(z, 0)$$

Causal evolution operator

$U(z,0)$: unitary operator (the norm of $|\Psi>$ is conserved), in general not directly integrable $\Longrightarrow$ approximations.

$U(z,0)$ can be directly integrated only when $H(\rho;z)$ and $\frac{\partial}{\partial z}H(\rho;z)$ commute. In that case the general solution is [3]:

$$U(z,0) = e^{-\imath \int_0^z H(\tau)\, d\tau}$$

$H(\rho;z)$ and $\frac{\partial}{\partial z}H(\rho;z)$ commute when:

- $V(\rho;z)$ does not depend on z, i.e. $V(\rho;z) = V(\rho)$(perfect crystal).
- $V(\rho;z)$ can be neglected (free space propagation).
- $H(\rho;z)$ is approximated by it potential term (phase object).

Three approximations are available in jems:

- Multislice method.
- Bloch wave method.
- Howie-Whelan column approximation.

Full jems version

The full jems version will be made available for the hands-on. Bring your laptop[21]!

[21] http://cimewww.epfl.ch/people/stadelmann/jemsv3_7624u2012.htm

- Gratias D. and Portier R.

  Time-like perturbation method in high-energy electron diffraction.

  Acta Cryst., A39:576–584, 1983.

- J.C. Humphreys.

  The scattering of fast electrons by crystals.

  Rep. Prog. Phys., 42:1825–1887, 1979.

- A. Messiah.

  Mécanique quantique, volume 1 and 2.

  Dunod, Paris, Paris, 1964.

- R. Shankar.

  Principles of Quantum Mechanics.

  Plenum Press, New York and London, 1994.